Vortex lines in layered superconductors. I. From 3D to 2D behaviour

Denis Feinberg

Classification
Physics Abstracts
74.20D — 74.60 — 74.70J

Vortex lines in layered superconductors. I. From 3D to 2D behaviour

D. Feinberg

Laboratoire d'Etudes des Propriétés Electroniques des Solides, Centre National de la Recherche Scientifique, associé à l'Université Joseph Fourier, B.P. 166, 38042 Grenoble Cedex 9, France

(*Received 25 January 1993, accepted 18 March 1993*)

Résumé. — On passe en revue les aspects fondamentaux des vortex dans les supraconducteurs lamellaires (naturels ou superréseaux artificiels), en mettant l'accent sur le rôle de l'anisotropie et des très courtes longueurs de cohérence. Ces composés se divisent en trois classes, de T_c croissants : chalcogénures, supraconducteurs organiques et oxydes de cuivre à haut T_c. La première partie de l'article résume les aspects quantitatifs dus à l'incorporation de l'anisotropie dans les descriptions 3D Ginzburg-Landau ou London du réseau de vortex : anisotropie des champs critiques et du réseau de vortex, coefficients élastiques et fusion. Ce type de modèle décrit une grande partie des propriétés des composés modérément anisotropes tels que Y : 123. La seconde partie concerne les systèmes lamellaires à couplage Josephson et identifie dans quels régimes les vortex présentent un caractère quasi-2D. Des effets qualitativement nouveaux comme les vortex Josephson, les vortex 2D, la transition de Kosterlitz-Thouless et le lock-in des vortex sont passés en revue. Cette analyse est adaptée aux composés du type Bi : 2212 et aux superréseaux, mais aussi à Y : 123 pour certains aspects.

Abstract. — The fundamental aspects of vortices in layered superconductors (natural or artificial multilayered materials) are reviewed, focusing on the role of anisotropy and very short coherence lengths. These materials divide into three classes, with increasing T_c's : chalcogenides, organic superconductors and high-T_c copper oxides. The first part of the paper summarizes the quantitative features of the vortex lattice, due to the incorporation of anisotropy in the 3D Ginzburg-Landau or London descriptions : anisotropy of critical fields and vortex lattice, elastic coefficients and melting. This kind of model describes most of the properties of moderately anisotropic compounds as Y : 123. The second part concerns the Josephson-coupled layered systems and identifies in which regimes vortices exhibit a quasi-2D character. Qualitatively new features as Josephson vortices, 2D vortices, Kosterlitz-Thouless transition and lock-in of vortices are reviewed. This analysis is adapted to compounds as Bi : 2212 or multilayers, but also to Y : 123 for some aspects.

Introduction.

More than 6 years after the discovery of superconductivity in copper oxides, great progresses have been achieved in the understanding of the macroscopic properties of these compounds. On the theoretical level, a satisfactory description of vortices in layered systems has been

developed, in parallel with more and more accurate and specific experiments on single crystals and epitaxial films. From this point of view the results are much more encouraging than those concerning the microscopic aspects, since up to now no consensus exists on a basic (conventional or not) high T_c mechanism. On the contrary, the well-developed phenomenology of vortex lines in layered materials shows both conventional aspects (with quantitative differences from « old » superconductors), as well as truly new features, characteristic of the strong anisotropy and very short coherence lengths of these materials.

THE MATERIALS. — Most usual superconductors (Pb, Al, Nb, A15 materials) possess a crystalline structure showing no anisotropy (mostly cubic symmetry). There exists also a family of oxide superconductors which are cubic perovskites and show relatively high T_c's : $Ba(Pb)BiO_3$ [1] and $Ba(K)BiO_3$ [2] ($T_c \leq 13$ K and 35 K respectively). One can also mention the Chevrel phases $M_yMo_6X_8$ ($T_c \leq 15$ K) [3], and the recently discovered A_3C_{60} compounds (A = K, Rb, cubic, $T_c \leq 33$ K) [4].

On the other hand anisotropic superconductors exist since the early 70's. First, the class of dichalcogenide of transition metals (TaS_2, $NbSe_2$ and others, as well as their intercalated compounds) is characterized by a moderate to strong anisotropy in the normal conductivity, increased by intercalation [5]. Secondly, the class of organic materials (Bechgaard salts), studied extensively by Jerome and coworkers, contains both quasi-1D compounds (family of $[TMTSF]_2X$), usually low T_c materials, and quasi-2D ones which reach $T_c = 10.4$ K with $(BEDT\text{-}TTF)_2Cu(CNS)_2$ [6]. One can also mention the intercalated graphite compounds as C_8K [7], while the C_{60} compounds may be considered as isotropic 3D organic materials. Third, high-T_c cuprates, with $La_{2-x}Sr_xCuO_4$, $YBa_2Cu_3O_{7-\delta}$ (noted Y : 123), $Bi_2Sr_2CaCu_2O_y$ (noted Bi : 2212) and $Tl_2Ba_2CaCu_2O_x$ (noted Tl : 2212) families, as well as parent compounds, are layered materials covering a large range of anisotropy. This range has been considerably enlarged by the synthesis of artificial multilayers of superconducting and insulating materials such as Y : 123/Pr : 123 [8], superconducting and metallic materials as Y : 123/(YPr) : 123 [9] or Bi : 2212/Bi : 2201 [10]. Let us also mention the wide area of multilayers obtained by alternating transition metals (V, Mo) with semiconductors (Si, Ge) and which can involve similar physics, although on scales much larger than the atomic distances. One may also quote the molybdenum bronze $LiMo_9O_{17}$, which is a low temperature quasi-2D superconductor but shows some analogies with the behaviour of the cuprates [11]. Therefore low dimensionality superconductors show a large range of T_c's but contain the highest T_c materials known up to now.

SIMPLIFIED ELECTRONIC STRUCTURE. — A phenomenological description relies on a small number of microscopic parameters, among which the electronic structure parameters [12]. Due to the extreme complexity of the realistic band structure and the lack of precise knowledge concerning the relevant quasiparticles at the Fermi level in the metallic state, it is useful to start with simple models. The first one is a simple free electron model with anisotropy, manifesting in a mass tensor. For an uniaxial layered material one takes a mass m_{ab} within the layers and m_c along the normal to the layers (c-axis). The resulting elliptical Fermi surface is characteristic of a weakly anisotropic material. The second one concerns strongly anisotropic structures and involves a tight binding parameter t_c across the layers. If $t_c \ll \varepsilon_F$, the Fermi energy in one layer, a new situation occurs where the Fermi surface is opened, close to a cylinder with modulated section. In this last case the effective mass m_c along the z-axis is such as $m_{ab}/m_c \approx (t_c/\varepsilon_F)^2$ and the electronic anisotropy can be extremely large.

Such descriptions oversimplify the actual layer stacking which characterizes for instance copper oxides and results in a very complex band structure. Although it is generally admitted that superconductivity directly originates from CuO_2 layers, other layers (CuO chains in

Y : 123 materials, BiO and TlO layers in Bi- and Tl-based materials) play certainly a role, not only in fixing the charge carrier density. For instance, superconductivity can be induced in metallic layers by the proximity effect and yield peculiar temperature dependences [13]. Some consequences on the upper [14] and lower [15] critical fields, and effective anisotropy [16] have been derived.

PHENOMENOLOGICAL MODELS. — Most of the theoretical analysis relies on the Ginzburg-Landau (GL) description and its generalizations. This model is purely phenomenological but can be obtained from the BCS microscopic description close to T_c, so that the order parameter is very small. It allows to calculate the spatial variation of the order parameter phase and amplitude in various situations. However one sometimes extends the results of the GL theory outside its range of validity, in order to obtain qualitative results. Fortunately, for extreme type II materials ($\xi \ll \lambda$, the field penetration length), which is the case for all high-T_c compounds up to now, one can replace the GL theory by the London model, except close to H_{c2} [17]. This electrodynamical description is valid down to scales of order ξ and holds in the full temperature range. It essentially provides the spatial variation of the phase.

Mass anisotropy is easily incorporated in the GL or London descriptions. The solution giving the flux lattice can be complicated for a general field orientation and reveals original properties (transverse magnetization, vortex chains), recently observed in experiments. The anisotropy of the vortex lattice has a dramatic influence on its elastic properties, themselves essential for their pinning properties as well as for thermal fluctuations of vortex lines. A large part of the theoretical work has been devoted to such properties, and a large part of experiments can be explained within this description, including the observation of the so-called irreversibility line. However, more work is necessary to decide whether this line indicates depinning of vortices, melting of the flux lattice or a vortex glass transition.

On the other hand, the GL model encounters an obvious limitation when the transverse coherence length is smaller than the layer spacing d. This occurs when the electronic parameter T_c is smaller than the mean-field gap Δ in a single layer. Then one usually replaces the 3D model by the Lawrence-Doniach (LD) description where the layers are coupled by Josephson tunneling [18]. The Josephson coupling parameter can be deduced from microscopic parameters in simple cases [19], but is usually set as a phenomenological parameter. It can be strongly influenced by proximity effects for instance [13-16].

The LD model matches the 3D model close enough to T_c such as the layered structure is unessential, but in the so-called quasi-2D regime, it brings new features on the vortex properties. Even in the 3D regime, some effects reminiscent of the layered structure appear, such as the lock-in transition of vortices [20-21].

The present contribution (I) presents a theoretical view of the intrinsic properties of vortices, at thermodynamic equilibrium and in the absence of extrinsic pinning. The discussion of pinning and critical currents will be the subject of the contribution by P. Manuel (II, same issue). On the other hand, irreversible phenomena involving magnetization measurements have been reviewed by Senoussi [22]. Section 1 is concerned with the anisotropic 3D description, and section 2 with the LD description and its consequences. The MKSA unit system will be used throughout the paper. The experimental aspects are not reviewed, only a few papers have been quoted. The list of references is of course not exhaustive.

1. The anisotropic 3D description.

1.1 THE 3D ANISOTROPIC GINZBURG-LANDAU AND LONDON MODELS. — Let us restrict ourselves to an uniaxial layered material, the crystallographic c-axis being parallel to the z-axis normal to the layers and the xy plane parallel to them. The GL free energy with a diagonal mass

tensor (m_a, m_b, m_c) (with $m_a = m_b = m_{ab}$) and order parameter $\Psi(\mathbf{r}) = |\Psi|(\mathbf{r}) \exp(i\phi(\mathbf{r}))$ takes the form ($F = F_S - F_N$) [23]

$$F = \int d^3\mathbf{r} \left[a(T) |\Psi|^2 + \frac{1}{2} b(T) |\Psi|^4 + \frac{\hbar^2}{4 m_{ab}} \left| \left(i\nabla_\parallel + \frac{2e}{\hbar} \mathbf{A}_\parallel \right) \Psi \right|^2 + \right.$$
$$\left. + \frac{\hbar^2}{4 m_c} \left| \left(i\nabla_z + \frac{2e}{\hbar} \mathbf{A}_z \right) \Psi \right|^2 \right] + \int d^3\mathbf{r} \frac{b^2}{2\mu_0} \quad (1)$$

where $\mathbf{A}_\parallel = (A_x, A_y, 0)$, $\nabla_\parallel = (\nabla_x, \nabla_y, 0)$ and $\mathbf{b} = \text{curl } \mathbf{A}$. The transverse coherence length are

$$\xi_{ab}(T) = (\hbar^2/4 m_{ab} |a(T)|)^{1/2}$$

within the layers, and

$$\xi_c(T) = (\hbar^2/4 m_c |a(T)|)^{1/2}$$

across the layers. The equilibrium order parameter is $\Psi_0 = (|a(T)|/b)^{1/2}$ with $a(T) = \alpha_0(T - T_c)$, T_c being the mean-field temperature. One has

$$\frac{\xi_{ab}}{\xi_c} = \sqrt{\frac{m_c}{m_{ab}}} = \Gamma \quad (2)$$

which defines the anisotropy parameter Γ.

In a weakly anisotropic metal, this continuum model holds if the Fermi energy ε_F is much larger than T_c or the mean-field gap Δ. Given the relation [23] $\alpha = (6\pi^2/7\zeta(3)) k_B T_c/\varepsilon_F$, this implies that the coherence lengths are at all temperatures much larger than the typical interatomic distances. This is in principle always valid close enough to T_c since the coherence lengths diverge at T_c. Moreover, in the strongly anisotropic case ($t_c \ll \varepsilon_F$), t_c must still be larger than $k_B T_c$.

At length scales much larger than the ξ's (i.e. if $H \ll H_{c2}$), one may set $|\Psi| = \Psi_0$ and the free energy per unit volume becomes a London free energy [17]

$$F = -\frac{B_c^2}{2\mu_0} + \frac{1}{2\mu_0} \int d^3\mathbf{r} \left[b^2 + \lambda_{ab}^2 |(\text{curl } \mathbf{b})_\parallel|^2 + \lambda_c^2 |(\text{curl } \mathbf{b})_z|^2 \right] \quad (3)$$

where $\lambda_{ab} = (m_{ab}/2\mu_0 \Psi_0^2 e^2)^{1/2}$ characterizes screening by currents flowing in the layers, i.e. $\mathbf{J}_\parallel = (1/\mu_0)(\text{curl } \mathbf{b})_\parallel$ and $\lambda_c = (m_c/2\mu_0 \Psi_0^2 e^2)^{1/2}$ characterizes screening by currents flowing across the layers, i.e. $\mathbf{J}_z = (1/\mu_0)(\text{curl } \mathbf{b})_z$. One has $\lambda_c = \Gamma \lambda_{ab}$, which indicates poorer screening by (weak) interlayer currents. The first term of (3) is the condensation energy, B_c is the thermodynamical critical field.

One must emphasize that screening of a field normal to the layers (hereafter denoted simply as « normal field ») involves only the London length λ_{ab}, while screening of a field parallel to the layers (« parallel field ») involves λ_{ab} when screened in the z-direction, and λ_c when screened along a layer direction.

Cuprate superconductors are extreme type-II materials, with $\kappa_z = \lambda_{ab}/\xi_{ab}$ of order 100 (for normal fields) and $\kappa_\parallel = (\lambda_{ab} \lambda_c/\xi_{ab} \xi_c)^{1/2} = \Gamma\kappa_z$ even larger (for parallel fields). Organic materials pertain to the same category, while dichalcogenides are less strongly type II and C_8K is type II for parallel field and type I for normal field.

The case of biaxial materials (showing a strong anisotropy in the layers or even quasi-1D)

involves three coherence lengths and three London lengths. For sake of simplicity we review here only the case of uniaxial materials, applicable to high-T_c cuprates if one neglects the weak *ab* anisotropy. Biaxial materials as organic compounds should reveal a richer phenomenology.

1.2 CRITICAL FIELDS H_{c1} AND H_{c2}. — The upper critical field is obtained from the linearized GL equations derived from (1) with the $|\Psi|^4$ term omitted [24]. The calculation follows from the isotropic case by a simple scaling and gives for a sample of size much larger than the ξ's [12]

$$H_{c2\,z} = \frac{\Phi_0}{2\,\pi\mu_0\,\xi_{ab}^2} \qquad H_{c2\,\parallel} = \frac{\Phi_0}{2\,\pi\mu_0\,\xi_{ab}\,\xi_c} \tag{4}$$

with $\Phi_0 = h/2\,e$, so that $H_{c2\,\parallel}/H_{c2\,z} = \Gamma$, superconductivity is less easily destroyed in parallel fields. For the general orientation, **H** making an angle θ with the z-axis, one has [12]

$$H_{c2}(\theta) = \frac{H_{c2\,z}}{\varepsilon(\theta)} \qquad \varepsilon(\theta) = \sqrt{\cos^2\theta + \Gamma^{-2}\sin^2\theta} \tag{5}$$

showing that $H_{c2}(\theta)\cos\theta \approx H_{c2\,z}$ if $\tan\theta \ll \Gamma$, and $H_{c2}(\theta)\sin\theta \approx H_{c2\,\parallel}$ if $\tan\theta \gg \Gamma$. The first scaling is exact if Γ is infinite and characterizes nucleation in decoupled layers (2D case). The scaling function $\varepsilon(\theta)$ and the crossover angle $\theta_0 = \tan^{-1}(\Gamma)$ are ubiquitous in the anisotropic 3D properties (see Eq. (4)).

The calculation of the first penetration field H_{c1} requires that of the free energy of an isolated and straight vortex line, as the solution of the London equation with a δ-function current source, which reads

$$\mathbf{b} + \lambda_{ab}^2\,\mathrm{curl}\left[\frac{\mathbf{m}}{m_{ab}}\,\mathrm{curl}\,\mathbf{b}\right] = \Phi_0\,\mathbf{l}\,\delta(\mathbf{r} - \mathbf{r}_0) \tag{6}$$

where **m** denotes the mass tensor, **l** the vortex line unit vector and $\mathbf{r}_0$ its position in plane normal to **l**. The standard derivation [17] gives for the symmetric directions

$$H_{c1\,z} = \frac{\Phi_0}{4\,\pi\mu_0\,\lambda_{ab}^2}\,\mathrm{Ln}\,\kappa_z \qquad H_{c1\,\parallel} = \frac{\Phi_0}{4\,\pi\mu_0\,\lambda_{ab}\,\lambda_c}\,\mathrm{Ln}\,\kappa_\parallel \tag{7}$$

so that $H_{c1\,z}/H_{c1\,\parallel}$ is of order Γ, which means that the parallel directions are « easy » for flux penetration. In the general case, the energy of a single vortex line making an angle φ with the z-axis is approximately [25]

$$F_v(\varphi) = \frac{\Phi_0^2}{4\,\pi\mu_0\,\lambda_{ab}^2}\,\varepsilon(\varphi)\,\mathrm{Ln}\,\frac{\kappa_z}{[\varepsilon(\varphi)]^{1/2}} \tag{8}$$

and first penetration occurs at the angle φ such as $G = F - \Phi_0 H\cos(\theta - \varphi) = 0$ and H is minimal. As a result **l** lies in the (**H**, **c**) plane, with $\tan\varphi \approx \Gamma^2\tan\theta$ and the first penetration field for a single vortex is [25, 26] (Fig. 1a)

$$H_{c1}(\theta) = \frac{\Phi_0}{4\,\pi\mu_0\,\lambda_{ab}^2}\,\frac{\mathrm{Ln}\,[\kappa_z/\varepsilon(\theta)]}{\sqrt{\cos^2\theta + \Gamma^2\sin^2\theta}}\,. \tag{9}$$

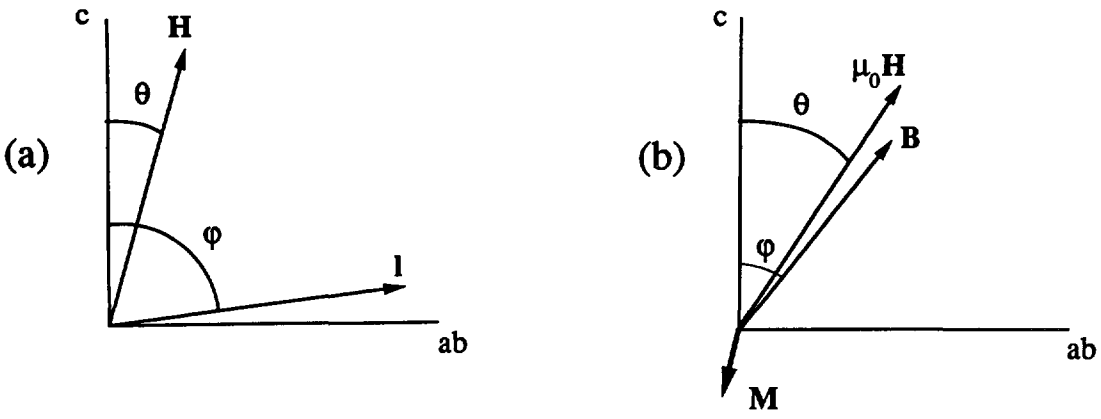

Fig. 1. — Vortex penetration in a tilted field. **H** : a) at H_{c1}, φ indicates the vortex direction ; b) for $H \gg H_{c1}$, φ indicates the direction of **B**.

In practice, for large Γ, vortex lines enter nearly parallel to the layers, due to the much smaller kinetic energy of the superconducting currents in this geometry.

One remarks that equations (5) and (9) (to logarithmic accuracy) can be written under the same form for both critical fields ($i = 1, 2$) [12]

$$\left(\frac{H_{ci}(\theta) \cos \theta}{H_{ci2}} \right)^2 + \left(\frac{H_{ci}(\theta) \sin \theta}{H_{ci\parallel}} \right)^2 = 1 . \tag{10}$$

However it has been recently shown for $\theta \neq 0$, 90° that it is slightly preferable to form a chain of vortices than an isolated vortex line [27]. The origin of this effect is the oscillating nature of the spatial field variation around a flux line, yielding an attractive interaction at a distance of order λ in the (**l**, **c**) plane containing the chain. In different words one can say that the currents stay nearly parallel to the ab plane, yielding a dipolar-like attraction of vortices tilted with respect to the c-axis. The free energy difference between a single line and a chain is maximum around $\varphi = 60°$ and increases with the anisotropy. It is of order of some % of the total energy.

1.3 STRUCTURE OF THE VORTEX LATTICE. — The structure of the flux line (vortex) lattice for $H_{c1} < H \ll H_{c2}$ is obtained by solving equation (6) where the right hand side is changed into $\Phi_0 \mathbf{l} \sum_i \delta(\mathbf{r} - \mathbf{r}_i)$, where the summation runs on the periodic flux line structure. The orientation of the unit vector **l** (parallel to the induction $\mathbf{B} = \langle \mathbf{b} \rangle$) is determined consistentdy as a function of the field direction (determined by the angle θ with the c-axis) and is very close to it unless H is less than a few times H_{c1} (at equilibrium).

The results in weak field ($H \geqslant H_{c1}$) yield an array of chains parallel to the (**l**, **c**) plane or (**H**, **c**) plane [28]. As the field increases above H_{c1}, the distance between chains decreases and a (distorted) triangular lattice is progressively recovered. Thus the chains can be observed only close to H_{c1}. Recently decoration of ab surface of untwinned Y : 123 crystals has revealed patterns which would correspond to cutting the chains of flux lines by the ab plane [29].

The dependence of the magnetization with field intensity and orientation has been studied in detail by Buzdin and Simonov [28]. A low fields, flux lines run approximately parallel to the layers but the magnetization remains very close to the z-direction (it results from in-plane

currents screening the normal field component). As the field is increased, flux lines quickly rotate towards the field. This results in an anomalous behaviour for the magnetization component parallel to the field : it first decreases above H_{c1}, then, depending on the field orientation, it may increase and exhibit a second maximum.

At higher fields ($H_{c1} \ll H \ll H_{c2}$), one obtains a distorted triangular lattice of Abrikosov vortex lines, oriented nearly parallel to **H** [30]. The side-to-base ratio b_2/b_1 of the triangles and the angle between the unit vectors $\mathbf{b}_1$ and $\mathbf{b}_2$ (in the plane normal to the flux lines) are

$$\frac{b_2}{b_1} = \frac{1}{2 \cos \beta} \qquad \tan \beta = \frac{\sqrt{3}}{\varepsilon(\theta)} \tag{11}$$

If $\tan \theta \ll \Gamma$, $\varepsilon(\theta) \approx \cos \theta$ and one easily verifies that the decoration pattern obtained by cutting the tilted flux lattice by an *ab* plane yields an approximately isotropic triangular lattice, just as if Γ was infinite (Fig. 2). Actually, for weak layer coupling the dominant interaction between vortices is the intralayer one, due to dominant screening of the normal field component, and stabilizes a nearly isotropic hexagonal lattice in any *ab* plane cut. These hexagonal lattices are shifted from layer to layer in order to form flux lines parallel to the field.

On the other hand, as θ gets close to 90° the flux lattice becomes more and more anisotropic. When $\tan \theta \gg \Gamma$, $\varepsilon(\theta) \approx 1/\Gamma$ and $b_2/b_1 \approx \Gamma \sqrt{3}/2$. Here screening of the parallel field component becomes dominant. For a field exactly parallel to the layers, the hexagonal lattice is compressed in the z-direction and expanded in the plane direction, with the same ratio as the ξ's or the λ's. Therefore, if the average vortex distance parallel to the layers is a_v, then the distance normal to them is $a_z \approx a_v/\Gamma$. This shows that at a field of order $H_0 = \Phi_0/2\ \mu_0\ \pi \Gamma d^2$, where d is the layer spacing, $a_z \approx d$ and the 3D London model must fail (see Sect. 2). The anisotropic vortex lattice has been observed by decoration in Y : 123 ($H \parallel ab$) [31]. Decoration experiments in 2 H-$NbSe_2$ in tilted fields provide a rough agreement concerning the distortion but do not yield the correct orientation [32]. Other experiments are needed, as well as refinements of the London theory.

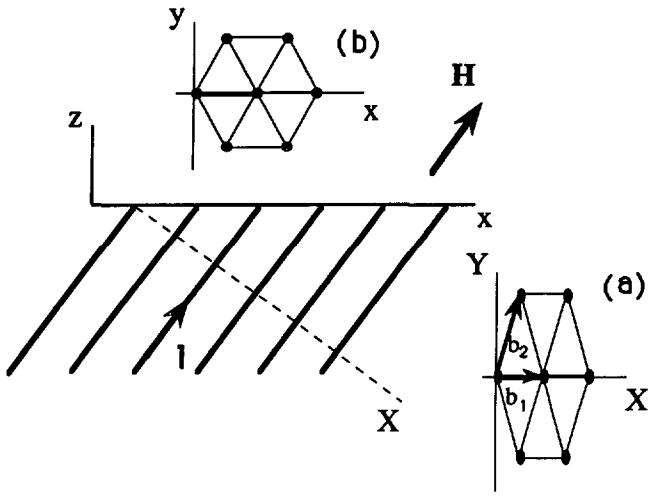

Fig. 2. — Tilted vortex lattice ($H \gg H_{c1}$). Insert a shows the distorted hexagonal cell in the plane *XY* normal to the vortices, and insert b the nearly isotropic cell of the lattice projected on the *xy* surface (*ab* plane).

For a vortex lattice oriented close to the layer direction, different vortex structures correspond to very slightly differing free energies. This can lead to very small shear moduli [33] and a chain structure has been proposed [34]. Other authors have found soft elastic modes, thus predicted an reconstruction of the triangular lattice when the *ab* direction is approached [35]. Actually, it is not clear which structure would replace the distorted triangular lattice. A possibility, suggested by decoration experiments on Bi : 2212 samples [36] is a lattice with a basis corresponding to chains embedded into a triangular lattice [37]. Besides, the formation of decomposed or combined lattices (two sublattices interpenetrating one parallel and one normal to the layers) has been suggested [38-39], but for very large anisotropies or field orientation very close to the *ab* direction (see Sect. 3). Observations report unusual chain patterns in Bi : 2212 samples (high anisotropy) [36], and zigzag patterns in 2 H-$NbSe_2$ (low anisotropy) [32]. This problem deserves more study and might reveal quite new kinds of vortex structures.

The anisotropy of the vortex lattice, associated with screening currents flowing preferentially close to the layer directions, has an important consequence : the magnetization has a component normal to the field (Fig. 1b). This was pointed out by Kogan who calculated the components M_c and M_{ab} (respectively normal and parallel to the layers) from the flux lattice free energy ($H \gg H_{c1}$) [40]

$$F_L = \frac{B^2}{2\,\mu_0} + \frac{\Phi_0 B \varepsilon(\theta)}{4\,\pi\mu_0\,\lambda_{ab}^2}\left[\mathrm{Ln}\,\sqrt{\frac{\eta B_{c2,z}}{B\varepsilon(\theta)}}\right] \tag{12}$$

where $\eta = 1.15$ for a triangular lattice. One obtains

$$M_c = -\frac{\Phi_0 \cos\theta}{4\,\pi\mu_0\,\lambda_{ab}^2\,\varepsilon(\theta)}\,\mathrm{Ln}\,\sqrt{\frac{\eta B_{c2,z}}{eB\varepsilon(\theta)}} \tag{13}$$

$$M_{ab} = -\frac{\Phi_0 \sin\theta}{4\,\pi\mu_0\,\lambda_c^2\,\varepsilon(\theta)}\,\mathrm{Ln}\,\sqrt{\frac{\eta B_{c2,z}}{eB\varepsilon(\theta)}} \tag{14}$$

where $\mathrm{Ln}(e) = 1$. If $\tan\theta \ll \Gamma$, M_{ab} is negligible and the magnetization is essentially normal to the layers.

To first order in the magnetization one obtains the reversible torque per unit volume, $T_\theta = M_c B_\parallel - M_{ab} B_z = \partial F/\partial\theta$, given by the expression [40]

$$T_\theta = -\frac{\Phi_0 B(1-\Gamma^{-2})\sin\theta\cos\theta}{4\,\pi\mu_0\,\lambda_{ab}^2\,\varepsilon(\theta)}\,\mathrm{Ln}\,\sqrt{\frac{\eta B_{c2,z}}{eB\varepsilon(\theta)}}\,. \tag{15}$$

It is zero for the parallel and normal orientations and exhibits a maximum at θ_M such as $\tan\theta_M \approx \Gamma$. One finds again the change of regime at an angle very close to 90° in case of strong anisotropy.

For moderate anisotropies this formula provides an accurate fit of experimental data and gives the value of the parameter Γ. For instance, values from 5 to 8 are found for $YBa_2Cu_3O_{7-\delta}$ with maximum T_c ($\delta \approx 0.1$) [41], but Γ increases rapidly with desoxygenation, as shown by Janossy *et al.*, attaining for instance $\Gamma = 20$ for $\delta = 0.35$ [42]. One can also measure independently the components of the magnetization [43].

For larger anisotropies as in Bi- or Tl-based systems, the results seem to be sample-dependent and give increasing values of Γ as the quality gets better. The value $\Gamma = 55$ was reported early for Bi : 2212 [44], but Γ may be larger in realty [45]. Accurate measurements meet the difficulty of sample alignment to less than 0.1°, but a more fundamental question is

raised by the validity of the 3D London model for such anisotropies. This point will be discussed in Part B. In addition, thermal fluctuations can influence the results [46]. Nevertheless the 3D interpretation yields a lower bound on Γ.

More generally, torque magnetometry, performed in the irreversible regime, and coupled to relaxation measurements, provide unique informations on pinning mechanisms and their anisotropy (twin boundaries for instance, or lock-in of vortices by the layers, see Sect. 4) [47].

1.4 THE SCALING TRANSFORMATION IN STRONG FIELDS. — The properties of the anisotropic flux lattice may be partially deduced in some cases from those of the isotropic one by a simple scaling of coordinates [26]. Such a scaling is obvious when the field lies along the crystal axis, but does not hold for a general orientation : in the latter case the direction of the local field **b** fluctuates and is only in average parallel to the flux line direction. However, an approximate scaling procedure exists which holds in high enough fields [48-49].

Let us rescale the coordinates x, y, z as $\tilde{x} = x$, $\tilde{y} = y$, $\tilde{z} = \Gamma z$. Then the vector potential and field transform as $\tilde{A}_x = A_x$, $\tilde{A}_y = A_y$, $\tilde{A}_z = A_z/\Gamma$ and $\tilde{b}_x = b_x/\Gamma$, $\tilde{b}_y = b_y/\Gamma$, $\tilde{b}_z = b_z$, and the Gibbs energy density $G = F - \mathbf{HB}$ obtained from equation (1) becomes [48]

$$G = \frac{1}{\Gamma}\int \mathrm{d}^3\tilde{\mathbf{r}}\left[a(T)|\Psi|^2 + \frac{1}{2}b(T)|\Psi|^4 + \frac{\hbar^2}{4\,m_{ab}}\left|\left(i\tilde{\nabla} + \frac{2e}{\hbar}\tilde{A}\right)\Psi\right|^2\right] +$$

$$+ \frac{1}{\Gamma}\int \mathrm{d}^3\tilde{\mathbf{r}}\left[\frac{\Gamma^2(\tilde{b}_x^2 + \tilde{b}_y^2)}{2\,\mu_0} + \frac{\tilde{b}_z^2}{2\,\mu_0} - \Gamma^2(\tilde{b}_x\tilde{H}_x + \tilde{b}_y\tilde{H}_y) - \tilde{b}_z\tilde{H}_z\right]. \quad (16)$$

The anisotropy has been transferred from the electronic part to the magnetic part of the free energy. There is no general solution, but in high enough field, the spatial modulation of **b** can be neglected (it is of order H_{c1}/H), so $\mathbf{b} \approx B$ and the magnetic part can be dropped. Such a procedure would be exact for κ infinite but is valid in a wide range of fields for extreme type II superconductors [48-49].

Equation (16) and the corresponding London free energy show that the vortex lattice derives from the isotropic case, with an effective field $\tilde{\mathbf{B}}$ such as $\tan\tilde{\theta} = \tan\theta/\Gamma$, thus much closer to the c-axis. In the rescaled coordinate frame, the screening currents run in the plane normal to $\tilde{\mathbf{B}}$, and the vortex density is fixed by the effective field intensity

$$\tilde{B} = B\varepsilon(\theta) \quad (17)$$

where the scaling function $\varepsilon(\theta)$ is given by equation (5). Going back to the original frame, it is straightforward to show that this results in the anisotropic vortex lattice obtained directly (see Sect. 1.3, Eq. (11)). More precisely, the second term of the free energy given by equation (12), corresponding to the first terrn of Γ (Eq. (16)) is simply obtained from the isotropic one by replacing B by $\tilde{\mathbf{B}}$, while the term $B^2/2\,\mu_0$ is unchanged. This leads to the expression (15) for the torque.

The scaling procedure also allows to obtain easily the magnetization close to B_{c2}, which may also be obtained directly [50]. In the isotropic case, M is proportional to Ψ^2 and is calculated in perturbations in $(B_{c2} - B)$. One obtains [24]

$$F = \frac{B^2}{2\,\mu_0} - \frac{(B_{c2} - B)^2}{2\,\mu_0\left[1 + (2\,\kappa^2 - 1)\,\beta_A\right]} \quad (18)$$

where $\beta_A = 1.16$ for the triangular vortex lattice. Equation (18) yields the magnetization through $B = \mu_0(H + M)$ and $H = \partial F/\partial B$. In the anisotropic situation the free energy follows from (18) by substituting B by $\tilde{B}$ and B_{c2} by $B_{c2,z}$ in the second term. Then one obtains for instance the torque [50-51]

$$T = -\frac{B_{c2}(\theta)[B_{c2}(\theta) - B](1 - \Gamma^{-2}) \sin(2\theta)}{2\mu_0[1 + (2\kappa^2 - 1)\beta_A]} . \tag{19}$$

A similar procedure can be used in the fluctuation region ($B > B_{c2}(\theta)$) to obtain the diamagnetic susceptibility and torque [51].

The scaling procedure is extremely useful for obtaining without much effort a high-field approximation to the elastic coefficients of the flux line lattice, from which the thermal fluctuations of the flux lattice follow [48]. As another consequence, pinning properties involving homogeneous disorder, and the corresponding critical currents, can be rescaled from the results in the isotropic case [48, 49]. Moreover, the angle dependence of resistivity, as well as critical currents, in single crystals and thin films should obey the scaling relation. Braithwaite *et al.* observed in Y : 123 the 3D scaling in a wide angular region [161]. However, due to other causes of anisotropy (pinning for instance), this is not always true. One must remark that, to make the difference with the two-dimensional ($B \cos\theta$) scaling (see Sect. 2), one needs to orient the field rather close to the layers (some degrees in Y : 123, some tenths of degrees in Bi : 2212). The two-dimensional scaling, widely observed in Bi : 2212 was explained by Kes *et al.* by a 2D behaviour of vortices (Γ infinite) [52]. However, very close to the layer direction Raffy *et al.* observed a 3D scaling [53]. As explained in section 2, the behaviour of Bi : 2212 and other very anisotropic materials can indeed be 2D or 3D depending on the conditions of the experiment. One must notice that, even in materials like $YBa_2Cu_3O_7$ which are essentially anisotropic 3D systems, some effects of the layered structure may appear close to the layer direction, for instance the lock-in transition (see Sect. 2.4), and mark a deviation from the 3D scaling.

1.5 ELASTIC COEFFICIENTS OF THE FLUX LATTICE. — The general problem of calculating the energy of any arrangement of curved vortices (specified by $\mathbf{r} = \mathbf{r}_i$ for a vortex line i) can be solved, thanks to the linearity of the London equations. Vortex line elements interact through the screening currents they create, up to a distance of order λ. While in the isotropic case two vortex elements $d\mathbf{r}_i$ and $d\mathbf{r}_j$ pertaining to lines i and j interact only through the scalar product $d\mathbf{r}_i \cdot d\mathbf{r}_j$, in the anisotropic case the interaction involves a tensor $f_{\alpha\beta}$

$$F = \frac{\Phi_0^2}{2\mu_0} \sum_{i,j} \sum_{\alpha\beta} \int dr_i^\alpha \, dr_j^\beta \, f_{\alpha\beta}(\mathbf{r}_i - \mathbf{r}_j) . \tag{20}$$

The explicit form of $f_{\alpha\beta}$ is given by Brandt [54, 55]. It allows to calculate the elastic coefficients of the vortex lattice, and also the barrier against cutting of vortices, which can be important for depinning and flux flow phenomena [56].

In the isotropic case, with field along the z-axis, one considers the small displacement $\mathbf{u}_i(z)$ of line i. Three-dimensional Fourier transform $\mathbf{u}(\mathbf{k})$ is taken, the longitudinal component k_z ranging from $-\infty$ to $+\infty$ and $\mathbf{k}_\perp = (k_x, k_y)$ running through the Brillouin zone of the triangular vortex lattice. Then the linear elastic energy of the lattice can be written as

$$F_{el} = \frac{1}{2} \int u_\alpha(\mathbf{k}) \, \Phi_{\alpha\beta}(\mathbf{k}) \, u_\beta(-\mathbf{k}) \frac{d^3\mathbf{k}}{8\pi^3} \tag{21}$$

$\Phi_{\alpha\beta}(\mathbf{k})$ is the elastic matrix. It is very important to notice that it is *dispersive*, i.e. it depends explicitly on the wavevector $\mathbf{k}$ [54, 57]. This is due to the long-range nature of the interactions between vortices. Those interactions extend to the length λ, usually much farther than the mean vortex separation $a_0 = (\Phi_0/B)^{1/2}$, if $H \gg H_{c1}$. The resulting *non-local* character of the elastic interactions, emphasized by Brandt, is an essential feature of the elastic theory of the vortex lattice. The general expression for $\Phi_{\alpha\beta}(\mathbf{k})$ can be found in references [54, 55].

Long-range deformations (of wavelength much larger than a_0) are conveniently described by the simplified expression

$$\Phi_{\alpha\beta}(\mathbf{k}) = [C_{11}(k) - C_{66}]\, k_\alpha\, k_\beta + \delta_{\alpha\beta}\left[C_{66}\, k_{ab}^2 + C_{44}(k)\, k_c^2\right] \tag{22}$$

with $k^2 = k_{ab}^2 + k_c^2$. Let us recall the usual meaning of the elastic moduli C_{11}, C_{66}, C_{44}.

The coefficient C_{11}, referred to as the bulk modulus, describes the rigidity of the vortex lattice against uniform compression. The coefficient C_{66} is the shear modulus. The tilt modulus C_{44} represents the stiffness against local rotation of the vortex lattice direction with respect to $\mathbf{B}$. Only C_{11} and C_{66} are relevant for a 2D lattice of point vortices. The simplified expressions for these moduli read (for $B \ll B_{c2}$ and $\kappa \gg 1$)

$$C_{66} = \frac{\Phi_0 B}{16\, \pi \lambda^2 \mu_0} \tag{23}$$

$$C_{11}(k) = \frac{B^2}{\mu_0} \frac{1}{1 + k^2 \lambda^2} \tag{24}$$

$$C_{44}(k) = \frac{B^2}{\mu_0}\left[\frac{1}{1 + k^2 \lambda^2} + \frac{1}{k_{BZ}^2 \lambda^2}\right] \tag{25}$$

($k_{BZ} \approx \pi/a_0 \approx (B/\Phi_0))^{1/2}$ is the radius of the Brillouin zone). Within the continuous approximation (22), only C_{11} and C_{44} are dispersive. C_{66} becomes dispersive at short scales.

These elastic moduli are the basic quantities which enter most theories of vortex pinning, and an essential feature is the dramatic dependence of the tilt and shear moduli on the anisotropy. We hereafter give the expressions for C_{11} and C_{44} for fields oriented along the c-axis or the ab planes of an uniaxial superconductor. The expressions of the elastic moduli for any orientation have been derived [35, 37, 58, 59]. One may also deduce them in the high field limit with the help of the scaling transformation [48].

First, if the field is along the c-axis, one has instead of (24) and (25) [60]

$$C_{11}(k) = \frac{B^2}{\mu_0} \frac{1 + k^2 \lambda_c^2}{(1 + k^2 \lambda_{ab}^2)(1 + k_{ab}^2 \lambda_c^2 + k_c^2 \lambda_{ab}^2)} \tag{26}$$

$$C_{44}(k) = \frac{B^2}{\mu_0}\left(\frac{1}{1 + k_{ab}^2 \lambda_c^2 + k_c^2 \lambda_{ab}^2} + \frac{\mathrm{Ln}\ \tilde{\kappa}}{k_{BZ}^2 \lambda_c^2}\right) \tag{27}$$

while C_{66} is not modified. In equation (27), $\tilde{\kappa}$ is a function of k_c and the various parameters [61]. The second term in C_{44} is the isolated vortex contribution and dominates at small B. It simply comes in this limit from the expansion of the single vortex line energy. All other terms in equations (23)-(27) are of collective origin.

The bulk modulus differs from the isotropic one only if longitudinal deformations are also present ($k_c \neq 0$), and is notably decreased only for very short wavelength k_c^{-1} On the other hand, the tilt modulus is dramatically diminished by the anisotropy : $k_{ab}^2 \lambda_{ab}^2$ being replaced in

the denominator by $k_{ab}^2 \lambda_c^2$, the tilt modulus is smaller by a factor Γ^2 for tilt angles smaller than $\tan^{-1} \Gamma$! Such an effect directly comes from the much longer range ($\approx \lambda_c$) of the interactions, allowing much larger distortions for the same amount of elastic energy. This feature has a crucial importance in the depinning properties and is also at the origin of a possible melting transition (next Sect.).

If the field lies along the *ab* plane, some elastic coefficients are dramatically modified. For instance, the shear modulus splits into a « hard » component C_{66}^h (shear direction along the *c*-axis) and a « soft » one C_{66}^s (shear direction parallel to the *ab* plane) [62] (Fig.3)

$$\frac{C_{66}^h}{C_{66}^s} = \Gamma^4 \qquad C_{66}^h = \Gamma C_{66} (B \,/\!/\, c)\,. \tag{28}$$

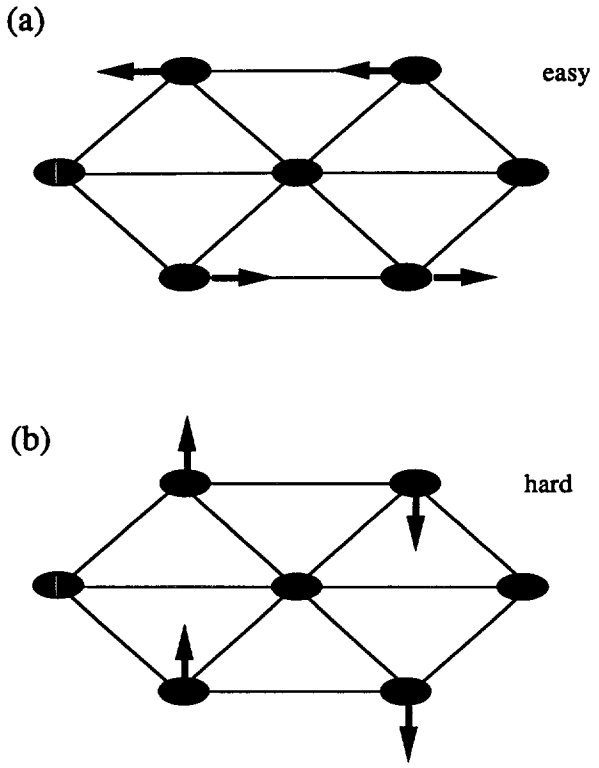

Fig. 3. — Easy (a) and hard (b) shear deformations of the anisotropic vortex lattice ($H /\!/ ab$).

The extreme softness along parallel shear makes the vortex lattice parallel to the *ab* planes already difficult to observe in Y : 123 [31]. In Bi : 2212, its coherence is probably destroyed by a small amount of thermal or quenched disorder.

On the other hand, the tilt modulus has also soft and hard components, respectively related to in-plane and out-of plane tilt [61]. The out-of plane tilt modulus has the peculiarity of being essentially dominated by the individual vortex contribution, itself proportional to the second angular derivative (in Γ^2) of the vortex line free energy (8) at $\varphi = 90°$. This is important for discussing for instance the lock-in transition (Sect. 2).

The above remarks allow to treat the problem of vortex cutting, as a function of the angle α between two vortex lines. In an isotropic superconductor their interaction energy vanishes when $\alpha = 90°$. Thus parallel vortex lines must bend in order to minimize their cutting energy. In an anisotropic superconductor ($\mathbf{B} \parallel \mathbf{c}$), the interaction vanishes only when $\alpha = 180°$ (if not, some component of currents in the *ab* plane remain). A full discussion of the problem shows that, due to the small tilt modulus, anisotropy makes globally cutting easier. This is an important feature for depinning of vortices in case of strong pinning [54].

Besides linear elasticity, one must also consider *plasticity* of the vortex lattice, especially in anisotropic superconductors : small elastic constants favour the formation of dislocations, either by thermal fluctuations or due to internal stresses generated by pinning and the Lorentz force (see Sect. 2) [54, 55].

Let us mention that the interactions between vortices close to a free surface are different from the bulk. This results in modified elastic properties [63], and may lead to different vortex arrangements [64].

1.6 THE MELTING TRANSITION. — The possibility of melting of the vortex lattice at temperatures much lower than T_c was first proposed by Nelson [65]. Fluctuations of the vortex lattice are indeed very large in cuprates, due to « high » temperatures and anisotropy, together with nonlocality, as emphasized by Brandt [66]. The application of the equirepartition principle allows to write down the average fluctuation of the vortex lattice deformation

$$\langle u_\alpha(\mathbf{k})\, u_\beta(\mathbf{k})\rangle = k_B\, T \Phi^{-1}_{\alpha\beta}(\mathbf{k}) \tag{29}$$

from which one obtains (using Eq. (22)) the mean square fluctuation $\langle u\rangle^2$ of a vortex position [60, 66]

$$\langle u\rangle^2 \approx k_B\, T \mu_0 \left(\frac{4\,\pi}{B \Phi_0^3}\right)^{1/2} \lambda_{ab}\, \lambda_c\,. \tag{30}$$

It is enhanced by the anisotropy (factor Γ), and by a factor B/B_{c1} compared to the local elasticity result of reference [65]. At high enough temperatures, long-range correlation will be lost and the vortex lattice *melts*. In analogy to crystal lattices, one can use the Lindemann criterium ($\langle u\rangle^2)^{1/2} \approx 0.15\, a_0$ to roughly evaluate the melting temperature (a_0 is the lattice spacing). This gives

$$k_B\, T_m(B) \approx 3 \times 10^{-3}\, \frac{\Phi_0^2}{\mu_0\, \Gamma \lambda_{ab}^2} \left(\frac{\Phi_0}{B}\right)^{1/2} \tag{31}$$

Far from T_c, this gives the dependence $B(T_m) \approx T_m^{-2}$, and close to T_c, $B(T_m) \approx (T_c - T_m)^2$ (Figs. 4-5). This is no more valid for very small B (close to H_{c1}).

This evaluation actually gives an upper limit to the theoretical melting transition. T_m will be decreased by the presence of defects, or by the presence of dislocations in the vortex lattice [66]. The melting line depends sensitively on the anisotropy : it is much lower in Bi : 2212 systems than in Y : 123. It can be physically characterized by the vanishing of shear stiffness. Above T_m, one has a « liquid vortex phase » characterized by the loss of long range correlations (Fig. 5). It is commonly believed that such a phase would be hardly pinned and could not sustain high currents without dissipation. This might not be true in case of very strong pinning. The possibility of melting at temperatures much lower than T_c is thus a specific aspect of anisotropic high-T_c superconductors and may put a fundamental limit on their potential applications.

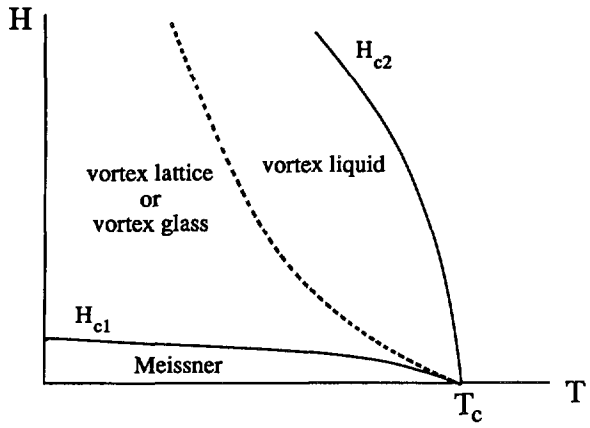

Fig. 4. — Schematic phase diagram for a 3D superconductor showing the melting line (dashed line) and the critical fields.

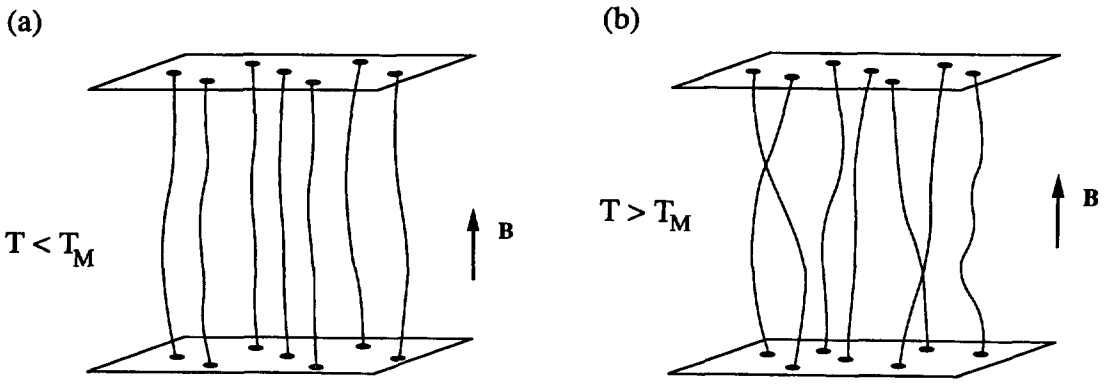

Fig. 5. — Thermal fluctuations for a 3D superconductor : a) $T < T_m$, b) $T > T_m$.

More technically, the melting problem has been approached through mapping wandering vortex lines onto the « world lines » of bosons (replacing the z coordinate by time) [65]. As a function of field and temperature, one may obtain a normal liquid or an « entangled » liquid of vortex lines above T_m. The latter phase bears some analogy with entangled polymers. Nelson and Seung argued that in the latter case, finite shear stiffness is obtained with a few pinning centers, and the viscoelastic response to an external current would allow finite critical currents in practice. However, the possibility of cutting (easy in cuprates) and recombination of vortices should strongly affect the viscoelastic properties of this phase [67]. A detailed theoretical discussion of melting in presence of disorder can be found in reference [68]. Also, the theory of melting has been reconsidered by Feigel'man by taking into account long range interactions and disorder [69], and a theory of pinning of the vortex liquid has been developed in reference [147].

Below the melting temperature, disorder already destroys long-range order of the vortex lattice. A *vortex glass* phase has been suggested, bearing no long range order but possessing shear stiffness, thus able to sustain critical currents [70]. The properties of such a phase are reviewed in reference [68]. It is characterized by the absence of an upper bound on the energy

barriers against motion of vortices. Hence this phase shows no resistance at low temperature and is truly superconductive. The existence of a true glass behaviour may be impeded by nucleation of dislocations in the vortex lattice which limit the barrier height. If energy barriers are limited, one is faced to the more traditional concept of thermal activation (Kim-Anderson theory and its refinements for high-T_c materials) and there is no true vortex glass. However a vortex glass behaviour may occur at low temperature where a large range of barriers is relevant. The debate is not so academic from the experimental point of view, since the vortex glass theory makes predictions concerning nonlinear current-voltage characteristics at low currents and at the glass-to liquid-transition, which seem to have been observed [71, 72]. On the contrary, the Kim-Anderson model, as well as the TAFF (thermally activated flux flow) mechanism, lead to ohmic characteristics.

Many experiments indeed show the existence of a line in the (H, T) plane, characterized by the onset of dissipation and reversibility of magnetization (see [54] for references and a critical discussion). This line is often called « depinning line », or « irreversibility line ». Depending on the experiment or on the quantitative criterium retained, its position may vary. It is not yet clear whether this line can be or not attributed to a (first order) melting or to a (second order) vortex glass transition, or simply to a collective depinning effect (which is not a phase transition). In fact, different phenomena may occur in a restricted range of temperatures or fields. Recently, a few experiments on untwinned Y : 123 crystals have perhaps answered the question. Safar *et al.* have found a first order transition in the very low current characteristic, in the dissipative regime [73].

On the other hand, Farrell *et al.* have detected a dissipation peak in a torque experiment, also slightly above the depinning threshold [74]. In both experiments the $B(T_m)$ variation is quadratic close to T_c, as predicted. Another evidence for a phase transition has been given by Charalambous *et al.* for H parallel to the ab plane [75]. Very recently other groups confirmed the existence of a melting transition [76, 77]. Hence it may be that, as temperature or field are increased, depinning first occurs, followed by a true melting transition. Figure 4 shows an oversimplified phase diagram for the vortex lattice.

2. Josephson-coupled layers and strongly anisotropic systems.

2.1 THE LD MODEL AND THE DIMENSIONAL CROSSOVER. — Lawrence and Doniach have proposed a phenomenological functional for a system of identical superconducting layers with spacing d and coupled by Josephson tunneling [18]

$$F = d \sum_n \int \mathrm{d}^2\mathbf{r} \left[a(T) |\Psi_n|^2 + \frac{1}{2} b(T) |\Psi_n|^4 + \frac{\hbar^2}{4 m_{ab}} \left| \left(i\nabla_\parallel + \frac{2e}{\hbar} \mathbf{A}_\parallel \right) \Psi_n \right|^2 + \right.$$

$$\left. + f_J \left| \Psi_{n+1} - \Psi_n \exp\left(\frac{2ie}{\hbar} \int_{nd}^{(n+1)d} A_z \, \mathrm{d}z \right) \right|^2 \right] + \int \mathrm{d}^2\mathbf{r} \, \mathrm{d}z \, \frac{\mathbf{b}^2}{2\mu_0} \quad (32)$$

where the order parameter $\Psi_n(x, y)$ is defined in layer n. The Josephson coupling f_J can be expressed in terms of an effective mass m_c, by $f_J = \hbar^2/4 m_c d^2$. This LD model has been justified microscopically by Bulaevskii [19], and it turns out that for a simple open Fermi surface, the « transverse » mass m_c is indeed related to the parameter t_c by $\hbar^2/m_c d^2 = t_c^2/\varepsilon_F$, thus $f_J = t_c^2/4 \varepsilon_F$ [12]. However, real systems possess a complicated electronic structure, and the analogy with Josephson junctions relies on the extremely short transverse coherence lengths (some Å). A real structure may be modelized by alternating superconducting and insulating layers, or by superconducting and metallic (normal) layers. The first case (SIS

structure) can be directly described by equation (32), but the second one (SNS structure) involves complications such as the proximity effect. It may be more conveniently described by a 3D anisotropic model, or, more generally, by 3D models involving a periodic modulation of the parameters [78]. Therefore, in the LD model studied here, the parameter m_c or the coupling f_J, as well as the effective anisotropy parameter $\Gamma = (m_c/m_{ab})^{1/2}$, must be considered as phenomenological.

Besides the parallel and transverse coherence lengths $\xi_{ab}(T)$ and $\xi_c(T)$, the LD functional defines a new length scale, obtained by comparing the parallel gradient term and the finite-difference term, respectively associated to the in-plane and the transverse stiffness of the order parameter. This shows that large differences $\Psi_{n+1}(\mathbf{r}) - \Psi_n(\mathbf{r})$ are allowed within a range $\lambda_J = \Gamma d$. This length thus characterizes the « shear stiffness » of the order parameter and is directly involved in lateral excursions of vortex lines parallel to the c-axis. λ_J is usually called « Josephson length », which may be misleading since it has not the same meaning as the Josephson screening length of a junction (see Ref. [92]). For example $\lambda_J \approx 60$-80 Å in Y : 123 and 600-1 000 Å in Bi : 2212, while $\lambda_J > \lambda_{ab}$ in more anisotropic materials, leading to exotic properties [38].

At lengths scales much larger than the ξ's, one can simplify the LD model and set $|\Psi_n| = \Psi_0 = (|a(T)|/b)^{1/2}$ This leads to a nonlinear LD functional for the phase ϕ_n of the order parameter, which is the equivalent for this model of the London functional

$$F = \frac{\Phi_0^2 d}{8\pi^2 \mu_0 \lambda_{ab}^2(T)} \sum_n \int d^2\mathbf{r} \left\{ |\nabla_\parallel \chi_n|^2 + \frac{2}{\Gamma^2 d^2} [1 - \cos(\chi_n - \chi_{n-1})] \right\} + \\ + \int \frac{\mathbf{b}^2}{2\mu_0} d^2\mathbf{r}\, dz \quad (33)$$

where

$$\chi_n(\mathbf{r}) = \phi_n(\mathbf{r}) - \frac{2e}{\hbar} \int_0^r \mathbf{A} \cdot \mathbf{dl} \quad (34)$$

defines the gauge-invariant phase.

One can define screening lengths λ_{ab} and λ_c, identical to those of section 1. These are large compared to the layer spacing and are hence insensitive to the layered structure. In other words, the electron density (or the order parameter amplitude $|\Psi_n|$) appearing in the λ's are quantities *averaged* on the whole sample volume, while superconducting electrons exist only within the layers n.

Due to the long scale of the field variation ($\lambda_{ab} \gg d$), the finite difference equations resulting from equation (33) may be replaced by 3D differential equations [79, 80]. However, the order parameter keeps variations at the scale d and the current sources in the layers are point vortices centered at $\mathbf{r}_{in}$ (in the « London » description). For instance the equation for normal flux reads [39]

$$\nabla^2 b_z = \frac{d}{\lambda_{ab}^2} \sum_n \left[b_z - \Phi_0 \sum_i \delta(\mathbf{r} - \mathbf{r}_{in}) \right] \delta(z - nd) \quad (35)$$

which immediately results in $B_z = \Phi_0 n_{2D}$, where n_{2D} is the density of 2D vortices per layer.

When the Josephson length is smaller than the parallel coherence length ($\lambda_J < \xi_{ab}(T)$), the system behaves as if the order parameter varied smoothly from one layer to another, and λ_J becomes unessential. The finite differences appearing in equations (32, 33) can be linearized, leading to an effective anisotropic 3D description. On the other hand, when

$\lambda_J > \xi_{ab}(T)$, the continuous description is not valid and new effects are expected. This dimensional crossover occurs at a temperature T^* defined by $\xi_{ab}(T^*) = \lambda_J/\sqrt{2}$, or $\xi_\perp(T^*) = d/\sqrt{2}$. It occurs provided the parameter $\rho = 2\,\xi_\parallel^2(0)/\Gamma^2 d^2$ is less than one. If $\rho < 1$, and $\xi_{ab}(T)$ shows a GL variation, one has $T^* = T_c(1-\rho)$. The theoretical values for ρ range from around 0.1 in Y : 123 to 0.001 in Bi : 2212 and are nearly zero in quasi-2D multilayers. This crossover can be observed in Y : 123, and deviations from the 3D London behaviour have indeed be observed in torque experiments below 80 K [81] (see Sect. 2.4). One must notice that dimensional crossovers may occur at lower temperatures (and thus be observed in more anisotropic materials), if concerning other physical properties. As will be emphasized in the following, 2D or 3D behaviour depends on the comparison of a length scale specific of the experiment with the Josephson length λ_J.

2.2 THE ZERO JOSEPHSON COUPLING CASE : 2D VORTICES. — This limiting case is interesting in many respects. First, it may be close to the situation of very large anisotropy, encountered in Bi : 2212 materials and artificial multilayers. Secondly, it leads to a linear GL or London problem which can be solved by standard methods. This (often called 2D) limit should not be confused with that of a real 2D superconductor (modelizing very thin films). Indeed, the electronic coupling is 2D but the magnetic coupling between vortices are 3D in nature.

The first calculation involving 2D vortices appeared in a paper by Efetov [82]. Buzdin and Feinberg expressed the free energy of a system of 2D vortices as the sum of two-body interactions [83] (see also Guinea [84], Clem [85], Fischer [86], as well as references [79, 80] where a « homogeinized » version of the 2D London equations was used)). The detailed field and current distribution has been given by Clem for a single 2D « pancake » vortex. The magnetic field is dipolar-like and extends to a distance of order λ_{ab} in the z-direction (Fig. 6b).

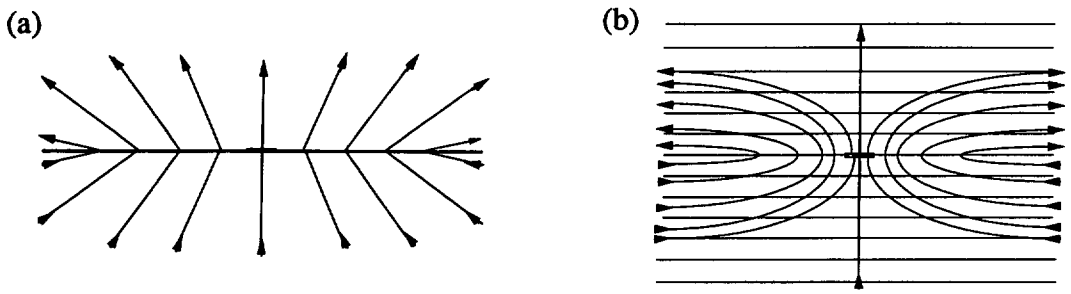

Fig. 6. — Single vortex and sketch of field lines : a) in a thin film b) in a multilayer superconductor without Josephson coupling : field lines are bent and are confined in a layer whose thickness is of order λ_{ab}.

In an infinite multilayer system, the free energy of a single 2D vortex diverges. On the other hand, in the same layer, the interaction of two vortices of same polarity is repulsive and *logarithmic* at any distance $R > d$ and ξ_{ab} (instead of exponential as for vortex lines in a 3D superconductor) [83]. If $d \ll \lambda_{ab}$, one has for an infinite stack of layers the interaction energy

$$F_{v\text{-}v} = -\frac{\Phi_0^2\, d}{2\,\pi\mu_0\,\lambda_{ab}^2}\,\mathrm{Ln}\,\frac{R}{\xi_{ab}} \tag{36}$$

The *total* energy of a *vortex-antivortex pair* is just the opposite. It is finite, the divergent parts

compensating each other. The logarithmic form at all distances is in contrast to the result for thin films where the interaction varies like $1/R$ for $R > \lambda_{ab}^2/d$ [87]. The multilayer result (36) is due to the screening currents induced in the other layers by a 2D vortex in a single layer. The direction of those currents is *opposite* to those occurring in the same layer [85]. For 2D vortices in different layers at a distance $z = nd$, one has the approximate forms [79, 85]

$$F_{v\text{-}v}(R, z) = \frac{\Phi_0^2 d^2}{8 \pi \mu_0 \lambda_{ab}^3} \operatorname{Ln} \frac{R}{\xi_{ab}} e^{-z/\lambda_{ab}} \quad (R \gg \lambda_{ab})$$
$$F_{v\text{-}v}(R, z) = \frac{\Phi_0^2 d^2}{8 \pi \mu_0 \lambda_{ab}^3} \frac{R}{\lambda_{ab}} \quad (z \ll R \ll \lambda_{ab}) . \tag{37}$$

Contrarily to (36), this interaction is *attractive*, expressing the fact that 2D vortices prefer to align along the z-direction. Compared to the in-layer interaction, it is weaker by a factor $d/\lambda_{ab} \ll 1$, but each vortex interacts up to a distance $z \approx \lambda_{ab}$ along the z-direction. The purely electromagnetic interactions between 2D vortices are thus *weak* and *long-range*, contrarily to the short-range electronic (Josephson) interactions. This allows in principle to calculate the total energy of any configuration of vortices and antivortices (Fig. 7). It is essential to notice that, due to the symmetry of the field distribution created by each vortex, such a configuration creates a field always *parallel* to the c-axis.

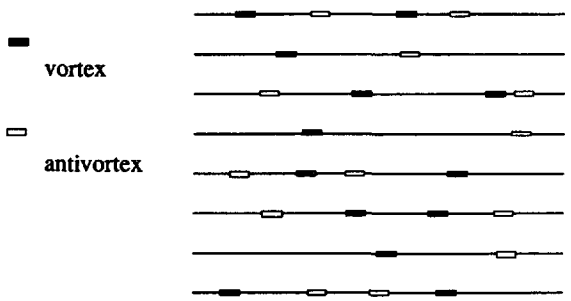

Fig. 7. — Example of a configuration of 2D vortices and antivortices (total induction is zero).

The London equations are easily solved for a field along the c-axis, and yield at equilibrium an Abrikosov lattice of 2D vortices [39, 85], in the layers, aligned along the z-direction. Curvature of the field lines is negligible since $d \ll \lambda_{ab}$, but may not be negligible in multilayers where d can be larger than 100 Å. The basic difference with a 3D superconductor is that continuous vortex lines leave place to fractioned lines of 2D vortices [67]. The origin of their alignment is the dipolar (magnetic) coupling between 2D vortices. The expressions for $H_{c1,z}$ and the intermediate field magnetization are similar to those of the 3D case (Sect. 1), as well as for the critical field $H_{c2,z}$. However, thermal fluctuations play here a crucial role (see Sect. 2.4).

In the case of a tilted field, the field component parallel to the layers cannot be screened in absence of Josephson currents, therefore it penetrates freely. The tilting of the field can be accomodated by a simple gauge transformation, and as a result the normal component H_z alone generates an Abrikosov lattice of 2D vortex lines *normal* to the layers [39] (Fig. 8). No tilting of the vortex lattice occurs, and all the equilibrium quantities (critical fields,

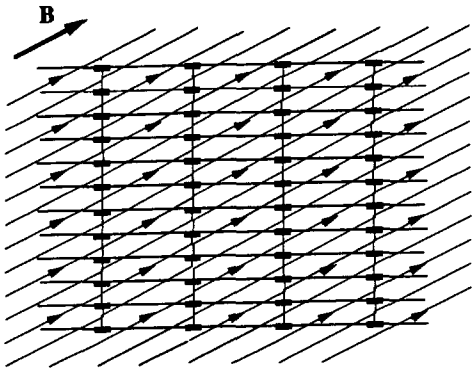

Fig. 8. — Abrikosov lattice of 2D vortices, generated by the normal field component, while the parallel one penetrates freely. (Arrows represent the direction of field lines.)

magnetization) are function of the component H_z, as would come from the 3D model by setting Γ to infinity (Eqs. (10, 13)). Many quantities (reversible and irreversible magnetization, vortex lattice decoration, resistivity, critical currents) reasonably obey in Bi : 2212 samples such a scaling law [52]. For a field making the angle θ with the c-axis, the measured values are those obtained from a normal field of strength $H \cos \theta$. However, deviations always occur close to the layer direction, and reflect the weak electronic interlayer coupling [53, 88]. This shows that the 2D model, though quantitatively valid in a wide range of parameters, is not physically correct and the effect of the Josephson coupling must be included. In practice, the Josephson coupling dominates the magnetic coupling beyond a distance r of order λ_J from a vortex core. If two 2D vortices in adjacent layers are shifted from each other by a distance R, a « string » of Josephson vortex will form if $R > \lambda_J$ [38, 39, 67, 79, 143] (Fig. 9).

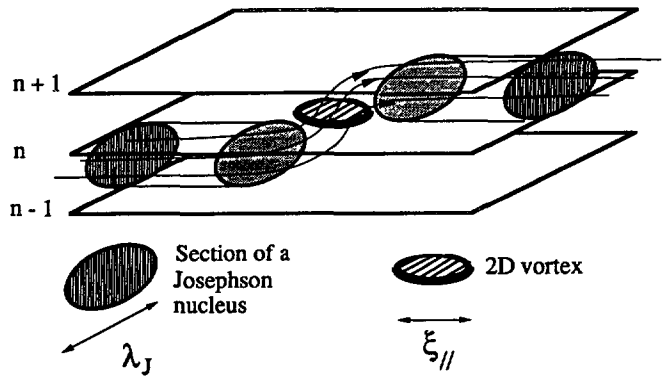

Fig. 9. — Structure of a kink : two portions of Josephson nuclei are linked by a 2D vortex. Note the difference in the sections, $\xi_{ab} < \lambda_J$. Some field lines are indicated.

2.3 THE VORTEX LATTICE : EFFECTIVE 3D DESCRIPTION AND BEYOND. — The tilted vortex lattice in the LD model has been studied for the quasi-2D regime ($T < T^*$) in references [38, 39, 85]. Reference [38] contains more detailed analytical calculations, using an approximate

linearization of the Josephson current, $\sin(\phi_n - \phi_{n-1}) \approx (\phi_n - \phi_{n+1})$, but keeping the finite-difference equations characteristic of the LD model. Flux lines are generated by tilted stacks of 2D vortices, aligned along a direction making an angle φ with the c-axis. In large enough fields, these vortex lines are nearly oriented along the field direction, as in the London case. What differs is the complex core structure of those lines, where three regions must be distinguished as a function of the distance r from a given vortex core center [38, 39] (Fig.10). At short length scales $r \leq \xi_{ab}(T)$, one finds the true 2D cores. At larger scales $\xi_{ab}(T) < r \leq \ell(\varphi)$, one has a nonlinear « nucleus » where interlayer currents are not small with respect to the critical Josephson current $J_c = \Phi_0/2\,\pi\mu_0\,\lambda_c^2 d$. The structure of this nucleus has been studied in detail by Carton [89] and Clem *et al.* [92, 146] in the case of parallel fields. This nucleus replaces in some way the GL core. Then, at scales $\ell(\varphi) < r \leq a_\lambda$, where a_λ is the vortex distance in a layer, the LD equations can be linearized to anisotropic 3D London equations. This is the effective 3D region where the layer structure is not relevant. The length $\ell(\varphi)$ limiting the quasi-2D and 3D regions is given by

$$\ell(\varphi) \approx \min\,(d \tan\varphi,\ \lambda_J) \tag{38}$$

where $d \tan\varphi$ is the mutual displacement of adjacent 2D vortices of a same vortex line. One can thus distinguish different angular regimes.

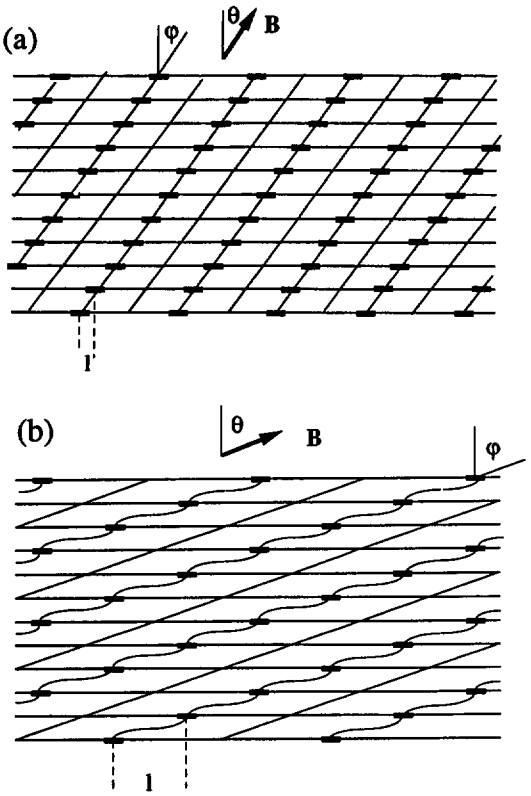

Fig. 10. — Vortex lattice in tilted field : a) $\tan\theta < \Gamma$, the regions between 2D vortices of the same line are the nuclei ; b) $\tan\theta > \Gamma$, $H_{/\!/} < H_0$ (see text), Josephson cores connect 2D vortices. The region between and far from 2D cores and nuclei is adequately described by 3D London equations. It disappears when $H_{/\!/} = H_0$.

i) $\tan \varphi \leqslant \xi_{ab}(T)/d$: the mutual displacement of adjacent 2D vortices is weak and the London model is applicable everywhere. It is modified to account for 2D cores by a « core constant » slightly different from the 3D one. For Y : 123 or Bi : 2212 compounds at low temperatures, the corresponding angular region ranges from $\varphi = 0$ to $\varphi = 45°$. It is smaller in artificial multilayers with larger d. The 3D London region between vortex cores exists provided $H_z \ll H_{c2,z}$.

ii) $\xi_{ab}(T)/d \leqslant \tan \varphi \lesssim \Gamma$: 2D vortex cores are displaced by more than their width, but not enough to leave place to strings of Josephson cores joining them. The expression of the vortex lattice free energy in this case is given in references [38, 39]. A simplified expression reads

$$F_L(\varphi) = \frac{B^2}{2\mu_0} + \frac{\Phi_0 B}{8\pi\mu_0 \lambda_{ab}^2}\varepsilon(\varphi)\,\mathrm{Ln}\,\frac{\Phi_0}{\pi d^2 \tan^2\varphi\,\varepsilon(\varphi)\,B} + \frac{\Phi_0 B_z}{4\pi\mu_0\lambda_{ab}^2}\times$$
$$\times\left[\mathrm{Ln}\,\frac{d\tan\varphi}{\xi_{ab}} + \alpha_{2D}\right]. \quad (39a)$$

It is similar to the 3D one, with the short range contribution modified to take into account the 2D character. The 3D London region between vortex « nuclei » exists provided $B_z \ll \Phi_0/2\pi(d\tan\varphi)^2$.

iii) $\Gamma \leqslant \tan\varphi$: in this case Josephson pieces of vortices fully develop, joining 2D vortices, the cores of vortex lines taking a « staircase » form (Figs. 9-10b). The limiting length $\ell(\varphi)$ is equal to λ_J, which means that from the point of view of 3D London picture, valid outside the nonlinear « nucleus », the steps appear as kinks of length λ_J and height d. If $\tan\varphi \gg \Gamma$, the vortex lattice free energy then takes approximately the form

$$F = \frac{B_\parallel^2}{2\mu_0} + \frac{\Phi_0 B_\parallel}{4\pi\mu_0\lambda_{ab}\lambda_c}\left[\mathrm{Ln}\sqrt{\frac{B_0}{B_\parallel}} + \alpha_J\right] + \frac{\Phi_0 B_z}{4\pi\mu_0\lambda_{ab}^2}\times$$
$$\times\left[\mathrm{Ln}\,\frac{\min(\lambda_{ab},\lambda_J)}{\xi_{ab}} + \alpha_{2D}\right]. \quad (39b)$$

The second term represents the interaction energy of the Josephson pieces of vortices, with the upper cutoff field $B_0 = \Phi_0/2\pi d\Gamma^2$ corresponding to all interlayer spacings being occupied by Josephson vortex nuclei. The constant α_J stands for the nonlinear nucleus contribution [92]. The third term corresponds to 2D vortices. One can remark that the angular condition to have Josephson pieces of vortices, and therefore to observe deviations from the 3D scaling law, is more easily fulfilled in experiments if Γ is not too large. Of course, a too small Γ is incompatible with the Lawrence-Doniach model since the Josephson coupling implies a substantial anisotropy.

More detailed expressions of the free energy can be found in reference [38]. At fields much smaller than the abovementioned limits, the effective London model is correct and vortex lines *at equilibrium* must be tilted, contrarily to the assumption of the 2D model [52] which assumes an Abrikosov lattice of vortices normal to the layers. One must underline than the tilting is uniquely due to weak *electronic* interlayer coupling, and this has important consequences. First, the interlayer coherence of the vortex lattice can be blurred by disorder, pinning or thermal fluctuations. Secondly, even if coherence of a tilted lattice is maintained, experiments may be unable to distinguish between a true 3D lattice and the 2D model. At equilibrium, one must sample the range $\tan\varphi > \Gamma$, and in this case the pinning and electrodynamic response of 2D and Josephson vortices show to be different from those of a 3D anisotropic superconductor [88, 101]. Also, the loose interlayer coupling was demonstrated by a recent experiment by

Safar *et al.*, showing out a decoupling of vortex motion on the two faces of Bi : 2212 crystal [145]. This and other experiments demonstrate that at high enough temperatures the electrodynamic response is that of decoupled 2D vortex lattices (see Sect. 2.6). The same property holds for pinning properties which are much closer to 2D than 3D behaviour (see the article by Manuel, same issue).

The case of parallel fields has been studied in more details [19, 89-93, 146]. If $H \ll H_0 = B_0/\mu_0$, one obtains a distorted Abrikosov lattice of vortices with Josephson-like cores (Fig. 11a). The GL core of section $\xi_{ab} \cdot \xi_c$ is replaced by the larger nucleus of section Γd^2. In small fields, interesting commensurability effects between the layer spacing and the vortex distance a_z may appear, and would manifest in jumps in the magnetization [95].

If $H > H_0$, the distance between vortices along the layers still decreases while their distance along the z-direction remains equal to d [93, 89]. In the LD model, there is no upper limit to such a stacking of Josephson vortices : their nuclei are squeezed, but the theoretical critical field $H_{c2\parallel}$ is infinite [94] (Fig. 11b). The tilted vortex lattice has been studied at H_{c2} by Minenko and Kulik [139]. In practice H_{c2} is limited by the paramagnetic effect [12], or by finite superconducting layer width [98]. If $T^* < T \leq T_c$ the angular dependence of H_{c2} is given by equation [10] (3D behaviour), and if $T < T^*$ the dependence is similar to that of thin films [157] and given by

$$H_{c2}(\theta)\left|\frac{\cos\theta}{H_{c2z}}\right| + \left(\frac{H_{c2}(\theta)}{H_{c2\parallel}}\right)^2 = 1 \tag{40}$$

where $H_{c2\parallel}$ is an effective critical field [12]. The crossover manifests itself in a rounding at $\theta = 0$, leaving place to a cusp below the crossover, and the two behaviours have been observed in cuprates [158-159]. Similar behaviour has been seen on the irreversibility line in Bi : 2212 [160], with a crossover temperature lower than 80K, thus different from T^*.

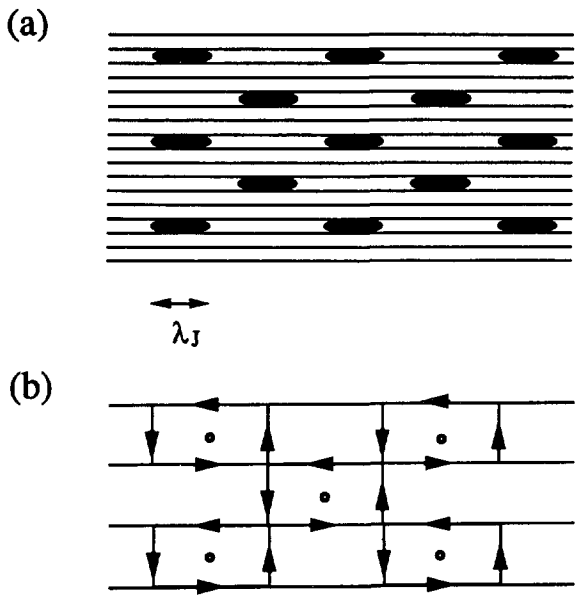

Fig. 11 — Josephson vortex lattice in parallel field : a) $H < H_0$ (hatched areas denote the section of Josephson nuclei) ; b) $H > H_0$, nuclei fill all the space, and circulating currents are represented.

An very peculiar situation arises when the field is tilted and such as $H_{\parallel} > H_0$. Then the interaction of 2D vortices in different layers favours stacking of kinks along the z-direction. In this case, a different vortex configuration is preferable : it involves a « combined » or « decomposed » lattice, made of two interpenetrating lattices of 2D vortices normal to the layers and a Josephson vortex lattice [38, 39, 142]. Indeed, within the London approximation, those two sublattices have no interaction energy, and the free energy difference between the tilted lattice and the combined one, coming from the interlayer interaction, varies like $1/\Gamma$. For $H = H_0$, 2D vortices occurring as kinks in tilted vortex lines happen to be naturally ordered in an isotropic sublattice, and for $H > H_0$ the combined lattice is favoured by the strong interaction of 2D vortices [38]. If the anisotropy is extreme ($\lambda_J > \lambda_{ab}$), case which might be realized in some bismuth and thallium-based compounds, as well as in multilayers, the combined lattice must form in a wide range of angles and fields. Its signature could be detected in torque experiments [38].

This question deserves further analysis, in relation with possible instabilities of the distorted hexagonal lattice, « frustrated » by the effect of field orientation close to the layers and strong anisotropy. More generally it would be interesting to make the link with the instabilities predicted in the London regime (Sect. 1). Experimentally, torque experiments could be a probe of such exotic vortex lattices but an extreme sensitivity is needed. The ideal probes are volume ones as neutron diffraction, which have recently given first results [132]. The difficulties are the weak field modulation (of order H_{c1}/H), and the difficulty to find a regime where vortices are nearly free from pinning but weakly fluctuating, so as to obtain a measurable structure factor. Other probes as μSR and NMR also encounter basic difficulties.

In the regime $T^* < T < T_c$ the properties of the vortex lattice are close to those of a 3D anisotropic one. However some differences exist and essentially come from a complex core structure. Let us simply consider the case of a vortex line parallel to the layers. The stable configuration corresponds to the center being between layers (Fig. 12a). The total size of the core is ($\xi_\perp$. $\xi_\parallel$), with $\xi_\perp > d$ and $\xi_\parallel > \lambda_J$. Within this region, the order parameter amplitude is weakened in the layers. A detailed variational calculation [21] shows that there also exists a nonlinear nucleus of size (d . λ_J) (like in the quasi-2D case) where Josephson currents are of the order of j_c. Outside this region, the phase differences between layers are small. Therefore the effective core in this quasi-3D regime has a complex structure, characteristic of a layered system. One can also consider the unstable configuration (Fig. 12b) where the vortex center sits on a layer. It is easy to see (and confirmed by calculations) that the nonlinear nucleus is larger, being spread on two interlayer spacings. As a consequence, the difference in core energy α_1 between the two configurations is of order

$$\alpha_1 \approx \left(\frac{d}{\xi_\perp (T)} \right)^2 = \frac{2}{\rho} \left(1 - \frac{T}{T_c} \right) \tag{41}$$

of the total vortex line free energy [21]. This result can be generalized to the vortex lattice provided $H \ll H_{c2}$. It contrasts with the exponential dependence found by expansions near H_{c2} or perturbative analysis [137, 148].

2.4 THE LOCK-IN TRANSITION AND INTRINSIC PINNING BY THE LAYERS. — In a true 3D anisotropic superconductor, with coherence lengths much larger than the atomic scale, vortices cannot align along a crystal direction unless the field also points along this direction. This is no more true in a layered structure, where vortices can « lock-in » onto the layer direction for a field tilted from the layers [20, 21]. The origin of the effect is the reduced free energy for vortex cores running along the layers. Two cases must be considered, depending on $T > T^*$ or $T < T^*$ (T^* is the crossover temperature defined in Sect. 2.1).

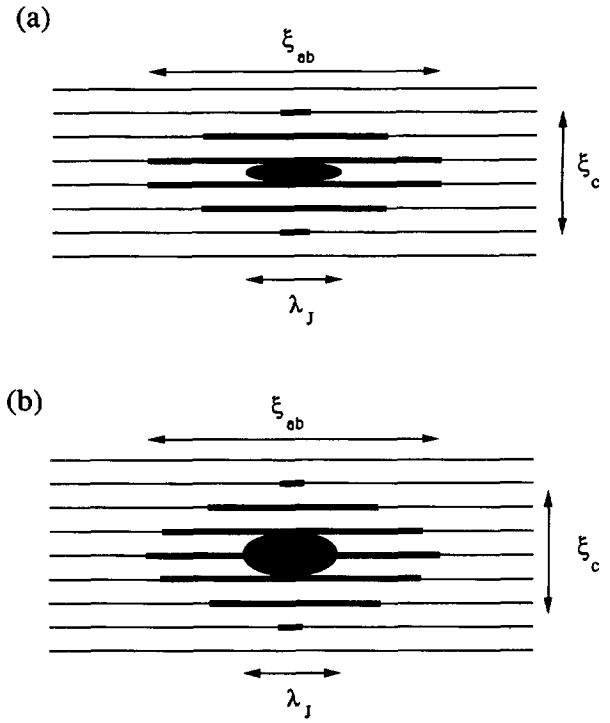

Fig. 12. — Structure of the core of a vortex parallel to the layers, showing the reduced order parameter (bold line) and the nonlinear nucleus (dark region). a) stable configuration ; b) unstable configuration.

Let us first consider the case $T \ll T^*$. When the transverse field component H_z is small, as shown by equation (39b), the interaction between 2D vortices vanishes : the free energy varies like cos φ instead of $\cos^2 \varphi$ in the 3D case (Eq. (12)) [38, 96-97]. As a consequence, 2D vortices vanish as soon as $H_z = H_\ell$, with

$$H_\ell = \frac{\Phi_0}{4\,\pi\mu_0\,\lambda_\parallel^2}\left[\mathrm{Ln}\,\frac{\min\,(\lambda_{ab},\,\lambda_J)}{\xi_{ab}} + \alpha_{2D}\right]. \tag{42a}$$

Thus, in the quasi-2D regime, the lock-in transition occurs at the frontier of the Meissner state for normal flux (Fig. 13). The lock-in angle is of order $H_{c1\,z}/H$. Moreover, it is very sensitive to demagnetizing fields which greatly enhance the component H_z in platelet samples or thin films with thickness s and length L : if the applied field H_a makes an angle θ_a with the c-axis, one has $\cos\,\theta_{a\ell} \approx (s/L)\cos\,\theta_\ell$, making the lock-in transition difficult to observe even in low fields [20, 99]. Moreover, the observation of a sharp normal flux penetration (by torque magnetometry for instance) suffers from the same difficulties as the determination of H_{c1}. The nucleation of kinks may be affected by the presence of defects and their interaction lead to a kind of critical state superimposed to the parallel flux lattice. To avoid those difficulties one must work in the reversible regime. Besides, at temperatures too close to T_c, thermal fluctuations may strongly modify the picture (see Sect. 2.6). An anomaly in the torque has been indeed detected by Farrell *et al.* [81] in Y : 123 below 80 K and attributed to lock-in by Bulaevskii [96]. However, this regime needs more discussion since it is outside the range of the true quasi-2D model (see Sect. 2.1).

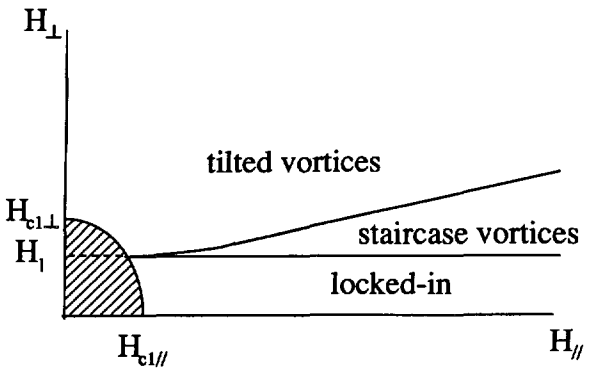

Fig. 13. — Phase diagram showing the Meissner and the lock-in regions, that of staircase vortices (tan $\varphi > \Gamma$) and that of the tilted vortex lattice (tan $\varphi < \Gamma$).

The model initially proposed for the lock-in transition [20] assumes that the core energy of a vortex parallel to the layers is periodically modulated along the z-direction, and uses for the London part of the free energy the expression from the 3D approach. This model is expected to be correct when the modulation α_1 of the core constant (to be included in the vortex free energy) is weak, i.e. in the regime $T^* < T < T_c$. The variational estimate of the temperature dependence of α_1 (Eq. (41)) contrasts with the exponential behaviour found in the similar problem of Peierls-Nabarro barriers for dislocations in crystals. The linear law comes from the nonlinear nucleus contribution (Josephson currents) and implies that a sizeable core energy modulation remains even close to T_c.

For a vortex lattice slightly tilted from the layer direction, the calculation proceeds through balancing the tilt energy involved by kink formation and the core energy gained by forming vortex segments parallel to the layers (Fig. 10b). The problem can be solved exactly for a sine core modulation and leads to Sine-Gordon kinks which disappear at a lock-in angle θ_ℓ. Here the kink length L_K is consistently calculated. It varies like $(\alpha_1)^{1/2}$ and turns out to be of the order of $\xi_{ab}(T)$ [21]. This result is due to the fact that, because of nonlocal elasticity, the « hard » tilt modulus $C_{44\perp} \approx \Gamma B H_{c1z}$ is dominated by the « single » vortex contribution [61]. The lock-in angle is defined by $H_z = H_\ell$, with

$$H_\ell = \frac{\Phi_0}{\pi \mu_0 \lambda_{ab}^2} \sqrt{\frac{2\,\alpha_1(\mathrm{Ln}\,\Gamma + \alpha)}{\pi}} \tag{42b}$$

It is possible to match the quasi-2D result (42a) to the quasi-3D result (42b) by noticing that $\xi_{ab}(T^*)$ is of order of λ_J, the kink length for $T \ll T^*$, so that (42a) and (42b) can be matched at T^* provided a phenomenological core barrier constant is defined at low temperatures. Therefore the modulated core energy treatment of the lock-in transition is roughly correct in the whole temperature range. Let us mention the more detailed analysis of the transition by Koshelev, in particular the possibility of kink wall formation [100].

In low fields and if demagnetizing effects are weak, the lock-in angle can be smaller than the angle marking the maximum of the London torque. In this case, the latter disappear and the torque maximum must be attributed to lock-in, giving only a lower bound to Γ. This points out the difficulty of observing the scaling (17) for large Γ's.

The lock-in manifests itself in a torque anomaly : when vortices suddenly lock onto the layer direction, their angle with the field increases and the torque is larger than the London torque

(Fig. 14). The position of the lock-in torque maximum θ_ℓ depends on the field, contrarily to the London maximum θ_m. it goes towards the layer direction as the field increases. Such effects have been observed recently in Tl : 2212 [101], but thermal fluctuations may modify the picture, as in measurements on Bi : 2212 [102].

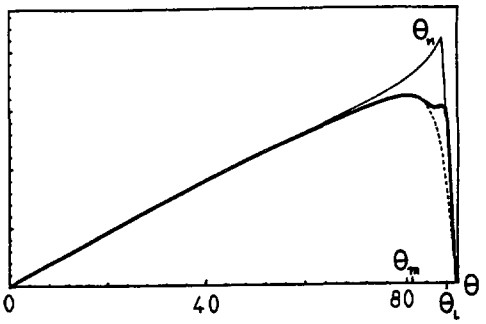

Fig. 14. — Typical torque curve : dotted line : London case ; bold line : lock-in correction ; thin line : 2D torque.

The energy E_K of the kinks is an important parameter since it controls their thermal activation. An estimate for Y : 123 leads to $E_K \approx 1.5 \times 10^3(1 - T/T_c)$ if $T \ll T^*$ and $E_K \approx 8 \times 10^3(1 - T/T_c)^{3/2}$ if $T > T^*$, leading to a kink energy of a few hundred Kelvins around T^*.

An important feature of layered materials is the possibility of intrinsic pinning of parallel vortices when a current is applied parallel to the layers, since in this case the Lorentz force opposes a strong core pinning force [140] (Fig. 15a). The intrinsic pinning energy can be as large as one tenth of the total vortex energy, and all vortices are pinned along their full length, which represents an extreme case of strong pinning (apart from slight distortions due to incommensurability effects). One can estimate the low temperature critical current associated to intrinsic pinning in low fields by assuming that, at equilibrium, fitting the cores between layers induces a negligible strain of the lattice (commensurate case). In that case the same Lorentz force is exerted on each vortex, on its full length. However, it is not likely that vortex lines pass rigidly from one interlayer spacing to another, since they would encounter an unstable configuration. Motion of vortices in the z-direction rather proceeds through *nucleation*

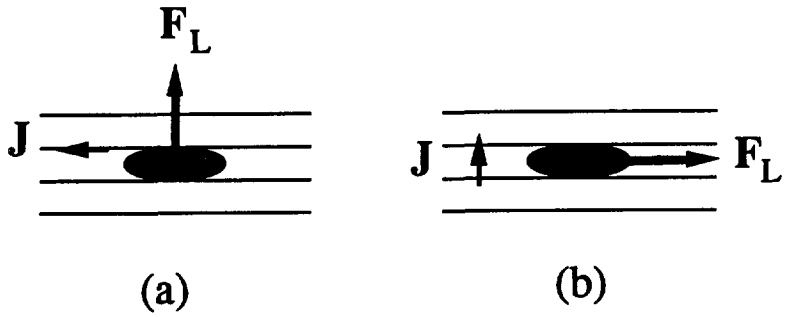

Fig. 15. — Lorentz force on a Josephson vortex : a) current in the layers, intrinsic pinning barrier (hard motion) ; b) current across the layers, very weak barrier (easy motion).

of pairs of kinks (Fig. 16). Such pairs might form coherently in many layers, so as to minimize the compressional energy (the tilt energy is mainly local and depends very slightly on such coherence). Indeed, such kinks locally look like 2D vortices, thus experience a force parallel to vortex lines, and once nucleated they move parallel to the layers. The nucleation energy is of order $2E_K$, and the pinning force per unit length is $f_p = E_K/dL_K$. Neglecting thermal activation, the critical current density is $J_c = E_K/dL_K \Phi_0$. Taking the expressions for E_K and L_K for $T < T^*$ and $T > T^*$, one finds

$$J_c = \frac{\Phi_0}{4\pi\mu_0 \lambda_{ab}^2 \lambda_J} \operatorname{Ln} \Gamma \qquad (T \ll T^*)$$
$$J_c = \frac{\Phi_0}{4\pi\mu_0 \lambda_{ab}^2 \lambda_J} 2\sqrt{2}\,\alpha_1 \qquad (T > T^*)\,. \tag{43}$$

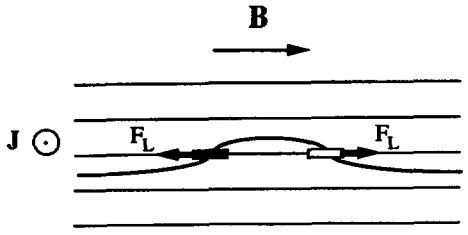

Fig. 16. — Nucleation of a kink and antikink (pair of 2D vortex and antivortex if $T < T^*$) on a Josephson line, and the Lorentz force in case of parallel current.

One verifies that J_c is always smaller than $J_p \approx \Phi_0/4\pi\mu_0 \lambda_{ab}^2 \xi_{ab}$, the depairing current in the layers. However values $J_c \approx 10^8$ A.cm^{-2} are theoretically possible. Assuming λ_{ab}^2 to be linear in T, the above evaluation yields $J_c \approx (1 - T/T_c)$ if $T \ll T^*$ and $J_c \approx (1 - T/T_c)^2$ if $T > T^*$. These low-temperature estimates must be corrected to take into account thermal activation of pairs of kinks and antikinks, important in practice.

At temperatures such as $k_B T \ll E_K$, high intrinsic critical currents can be maintained within the lock-in region, thus tolerating a misorientation of the field less than $90 - \theta_\ell$ with respect to the layers. However, thermal activation or kinks, or nucleation of kinks at defects can substantially lower these ideal values. Moreover, defects like twin boundaries or oxygen vacancies may help nucleation of kinks [140] but oppose barriers to their motion. In that case the critical currents may be limited by intrinsic or extrinsic barriers depending on which one is larger.

On the other hand, glide of vortices parallel to the layers is easy at low temperature where, in absence of true vortex core, the friction due to extrinsic defects is very weak (Fig. 15b). Thus critical currents flowing across the layers are very small. Contrarily to the above intrinsic critical currents, those currents must increase with temperature, since the larger core overlapping the layers increases the extrinsic pinning. Due to easy entrance of vortex cores between layers, the irreversibility measured by magnetization for fields parallel to the layers is weak and cannot reflect the intrinsic pinning, apart from special sample geometries [22]. On the other hand, direct measurements of J_c yield values in agreement with the above estimates [141], but in thin films where size effects may modify the picture. Also, the lock-in transition has been detected by transport measurements as a sharp drop in the dissipation, at a

temperature close to T_c in Y : 123 [103]. The remaining small dissipation is probably due to thermal activation of kinks in this case (see below).

The problem of dissipation in the parallel geometry, due to motion of Josephson-like vortices, has been considered by various groups. Clem and Coffey calculated the viscous drag coefficient for motion parallel to the layers, as well as the vortex inertial mass, and found results analogous to those of the anisotropic GL theory, where the size ($\xi_{ab} \cdot \xi_c$) of the vortex core must be replaced by ($\lambda_J \cdot d$) [146]. This is essential in order to know whether underdamped fluxon motion is possible in layered high-T_c superconductors (such effects would be an unambiguous proof of the presence of planar Josephson junctions between CuO_2 layers).

On the other hand, in a series of papers, Ivlev, Kopnin *et al.* studied dissipation due to vortex motion across the layers (intrinsic pinning), by thermal activation of vortex kinks. In parallel fields and close to H_{c2} [148], for $T^* < T < T_c$, the barrier for depinning varies as $U \approx 1/J$ at low currents, yielding nonlinear resistivity and the critical current goes like $\exp(-(\xi_c/d)^2)$. The contribution of kinks in a slightly tilted field was treated in reference [149] ($H \leq H_{c2}$, $T^* \leq T < T_c$), showing that the effect of intrinsic pinning vanishes at small tilting. At lower fields and parallel fields, activation of individual kinks or bundles leads to a barrier $U \approx H^2 J^{-2}$ at small currents [150]. In tilted fields, the 3D scaling (see Sect. 1.4) is obeyed, and is replaced by the $B \cos \theta$ scaling in the quasi-2D case [151-152], with about no dependence on the current direction in the layers [152], as found in experiments [153]. To end this brief enumeration, let us mention the calculation of quantum creep, due to quantum tunneling of a vortex core across a defect. This phenomenon offers a new example of a macroscopic quantum effect. It is possible below a field and current-dependent crossover temperature, due to the very small core (or nucleus) dimension. The phenomenon was theoretically studied for intrinsic pinning by the layers [154] as well as extrinsic pinning [155], and some observations have been made in Y : 123 [170].

More experiments are required to study intrinsic pinning and decide whether it may be important for applications. Let us stress again that the lock-in effect is not restricted to the quasi-2D regime $T < T^*$, but that, due to the peculiar core structure even above T^* (Fig. 12), it has been observed close to T_c in $YBa_2Cu_3O_7$ [103]. More recently, lock-in and strong anisotropy were observed in $(BEDT\text{-}TTF)_2Cu(SCN)_2$ [171, 172].

2.5 THERMAL FLUCTUATIONS : IS THERE A KOSTERLITZ-THOULESS TRANSITION ? — The 2D character of vortices in the low-temperature regime of Josephson-coupled layered superconductors soon raised to the possibility of a Kosterlitz-Thouless-Berezinskii transition [104-109], as in 2D superfluids and thin amorphous superconducting films. This transition originates from the unbinding of thermally excited vortex-antivortex pairs (Fig. 17a) and corresponds to the real transition temperature, as measured by transport experiments. From the experimental point of view in cuprates superconductors, evidences have been obtained in massive samples or thin films [110-114] as well as in artificial Y : 123/Pr : 123 multilayers [115]. They show below T_{KT} the nonlinear characteristics $V \approx I^{a(T)}$ where $a(T)$ exhibits an universal jump from 3 to 1 at T_{KT}, due to current-induced unbinding of pairs (the universal jump is not confirmed in all experiments). On the other hand, an exponential temperature variation of the resistivity appears above T_{KT} [156].

Theoretically, two objections have been raised against such a behaviour : first, in the case of vanishing Josephson coupling f_J, the problem is not strictly bidimensional, owing to the 3D electromagnetic interactions of vortices (see Sect. 2.2). Secondly, the Josephson coupling suppresses the logarithmic interactions of 2D vortices. Let us consider these two problems successively.

If $f_J = 0$, a vortex and antivortex interact logarithmically in the same layer [83]. If one neglects the (small) interlayer interaction, one obtains the Kosterlitz-Thouless temperature

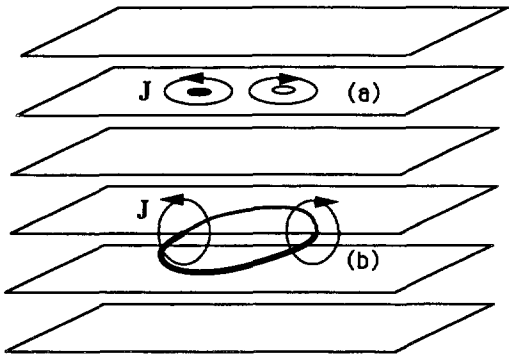

Fig. 17. — Thermal excitations of a weakly coupled layered superconductor : a) pair of 2D vortex-antivortex ; b) fluxon loop between two layers (the bold loop indicated the fluxon nucleus). Circulating currents are indicated.

$T_{KT} = V_0(T_{KT})/4$, thus

$$T_{KT} = \frac{\Phi_0^2 d}{8 \pi \mu_0 \lambda_{ab}^2(T_{KT})} \tag{44}$$

This already gives for Bi : 2212 $(T_{c0} - T_{KT})$ of order a few degrees. However, the screening effect of the bath of thermally activated vortex-antivortex pairs in other layers must be evaluated. This was done recently by a renormalization group analysis by Horovitz [116], and by Scheidl and Hackenbroich [117], who showed for a low density of excited pairs that a modified KT transition takes place at T'_{KT}, with $T'_{KT} < T_{KT} < T_{c0}$. Hence the tridimensional screening of the logarithmic interaction is slightly stronger than in the usual 2D case.

One should remark that the simple result (44), together with the usual scaling relations [104-

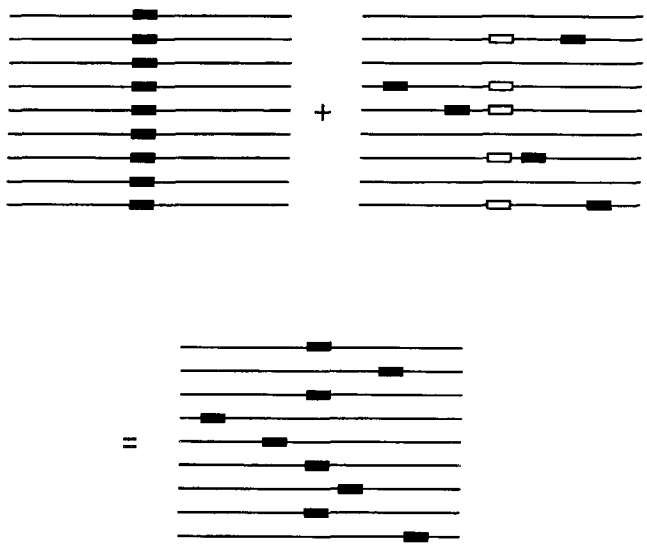

Fig. 18. — Evaporation of a single vortex line by thermal excitation of vortex-antivortex pairs superimposed onto the line.

109], holds only in the case of a small vortex density. This density is controlled by the core energy, itself of order $(\Phi_0^2 d/4 \pi \mu_0 \lambda_{ab}^2) \alpha$. If, as seems to be the case in Y : 123/Pr : 123 multilayers with a few unit cells per Y : 123 layer, T_{KT} is much smaller than T_{c0}, then the low density approximation becomes questionable. An alternative to the usual KT scenario could be the melting of a « vortex crystal », as proposed by Gabay and Kapitulnik [173].

Another approach of the problem consists in examining the stability against thermal fluctuations of a single vortex line, made of 2D vortices aligned along the z-axis. This problem was considered in references [118-121], and it comes out that the line « evaporates » due to very short wavelength distortions, for which the elastic coefficient is much reduced compared to a 3D superconductor. The temperature of evaporation T_{ev} was calculated [118], and turns out to be exactly equal to T_{KT} in a simple layered system. Indeed, displacing one 2D vortex is equivalent to adding to a straight vortex line a vortex-antivortex pair in a layer n, the antivortex cancelling the vortex in the same layer (Fig. 17) [83,86]. As shown in reference [117], at large distances the added pair has zero interaction with the vortex line, so it unbinds at the same temperature T_{KT} as in absence of the line.

The problem of the Josephson interaction is more difficult. Actually, when the vortex-antivortex separation R exceeds the Josephson length λ_J, a pair of Josephson vortices develop between them and the logarithmic interaction (36) (with opposite sign) is replaced by a linear one [79, 80, 122] (Fig. 19). Thus, for very large anisotropy ($\Gamma \gg 1$), the KT scaling remains valid at length scales shorter than λ_J. This upper limit can be raised by thermal fluctuations partially washing out the phase (Josephson) coupling [80]. It results that KT transition is possible in quasi-2D superconductors as Bi : 2212 or multilayers ($\lambda_J \gg \xi_{ab}$). Its observation in Y : 123 which is weakly anisotropic is questionable but a smeared KT transition is still possible [130]. However the situation is more complicated, since another kind of thermal excitation exists, made of elementary Josephson vortex loops, or « fluxons » situated between two adjacent layers (Fig. 17b). Such an excitation was considered by Friedel [122], Korshunov [123] and Horovitz [116]. Considered alone, it leads to a transition temperature T_f above which the Josephson coupling is renormalized to zero. Following Korshunov and Horovitz, one has $T_{KT} < T_f$, so that T_{KT} would be irrelevant and the transition at T_c has a 3D nature, with $T_{KT} < T_c < T_f$. Below T_c, f_J is finite and one has no free 2D vortices, while, above T_c, f_J is renormalized to zero and one has a gas of free 2D vortices. Only in the case of exponentially small Josephson coupling T_c becomes close to T_{KT} and the transition is of Kosterlitz-Thouless type [116]. However, as explained previously, the concept of (bound) 2D vortices retains an *approximate* validity at lenght scales smaller than the *renormalized* λ_J (going to infinity at T_c).

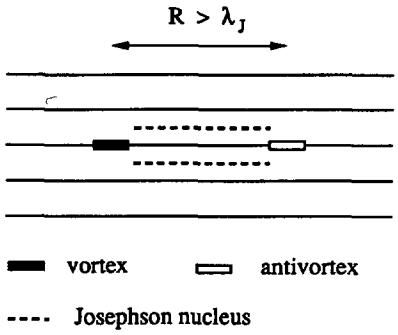

Fig. 19. — Vortex and antivortex in the same layer, connected by two pieces of Josephson vortices of opposite polarity.

From the point of view of vortex evaporation at low inductions, in the case of finite Josephson coupling, one also obtains a transition at $T_{ev} > T_{KT}$. Bulaevskii *et al.* have calculated the magnetization, taking into account thermal fluctuations, and fitted experimental data on Bi : 2212 samples [121]. Fischer [130] has also discussed the effect of an external field on the KT transition.

The problem of the actual T_c in layered structures is of peculiar interest owing to the very wide range of couplings realized in multilayers, for instance alternating Y : 123 (of thickness d_0) and the semiconducting Pr : 123 (of thickness $d - d_0$) [8], or Bi : 2212 and the low-T_c Bi : 2201 [10]. In the first case, substantial decrease of T_c was found as the thickness of the PrBCO layer was increased [124]. The probable explanation is a Kosterlitz-type transition [116, 125, 156], but other reasons as hole filling by charge transfer [126] have been proposed. A proximity effect, proposed in reference [144], seems unlikely due to the small transverse coherence length compared to the interlayer spacing [115]. One striking result is the saturation of T_c to a nonzero value when the superconducting layer separation $(d - d_0)$ becomes very large (more than 100 Å in Y : 123/Pr : 123) [127]. It is even believed that one unit cell of YBCO is superconducting [128], with a transition temperature $T_c = T_{KT}$, i.e. the saturation temperature would correspond to the real KT scenario [116]. In the general case, for a SIS structure, one expects Ln $(f_J) \approx (d - d_0)$. In this case the theory of reference [116] is in agreement with experiments. One must however take into account the finite (and often small) number of layers in real multilayers, the total thickness being smaller than λ_{ab}. This may strongly affect the results concerning the role of 3D screening in the KT transition.

2.6 ELASTIC PROPERTIES AND THE MELTING TRANSITION. — Let us first recall the results for truly 2D melting, valid for sufficiently thin films [129]. Melting is then characterized by a vanishing shear coefficient C_{66}, due to unbinding of *dislocation pairs,* at a temperature determined (in intermediate fields) by $k_B T_M^{2D} = C_{66} a_0^2/4\pi$ where a_0 is the lattice spacing, thus

$$k_B T_M^{2D} = \frac{1}{4\pi\sqrt{3}} \frac{\Phi_0^2 d}{8\pi\mu_0 \lambda_{ab}^2(T_M^{2D})} \tag{45}$$

This temperature can be much smaller than the zero-field T_{KT}. Above T_M^{2D}, the *positional* order is lost but the *orientational* order is preserved, one has then an *hexatic* phase, destroyed at T_H where an isotropic 2D vortex liquid is recovered.

The generalization to an infinite stack of layers (zero Josephson coupling) where the field is normal to the layers follows the same line as the zero-field KT transition, by replacing 2D vortex-antivortex pairs by dislocation pairs [79]. They interact logarithmically, and their interaction is much weaker if they sit in different layers. The effect of 3D vortex interaction has not yet been included, but one expects a quasi-2D melting temperature $T_M^{Q\,2D}$ close to T_M^{2D}.

In case of finite Josephson coupling the situation is more complicated. Elastic coefficients may be calculated within the 3D anisotropic theory with large Γ values. However such a *continuum* picture must fail for short wavelength distortions, especially along the z-axis. This is obvious from expression (27) where in the limit $\Gamma \to \infty$, $\lambda_c \to \infty$, $C_{44} = 0$ unless $k_{ab} = 0$. For small Γ, one can indeed modify the calculation of the elastic coefficients by keeping the finite-difference nature of the interlayer couplings (see Eqs. (32, 33), but replacing $\sin(\phi_n - \phi_{n+1})$ by $(\phi_n - \phi_{n+1})$. Following Bulaevskii *et al.* [38] and Glazman, Koshelev [131], this approximation preserves the discrete nature of the system and allows a *linear* theory of the quasi-2D vortex lattice deformations.

Let us first consider the case **H**$/\!/$**c**. The tilt coefficient is especially affected, for large values

of k_c. One has instead of (27)

$$C_{44}(k) = \frac{B^2}{\mu_0} \frac{1}{1 + k_{ab}^2 \lambda_c^2 + \tilde{k}_c^2 \lambda_{ab}^2} + \frac{\Phi_0 B}{8 \pi \mu_0 \lambda_{ab}^2} \left[\frac{1}{\Gamma^2} \text{Ln } \tilde{\kappa}_1 + \frac{1}{\lambda_{ab}^2 \tilde{k}_c^2} \text{Ln } \tilde{\kappa}_2 \right] \quad (46)$$

where $\tilde{k}_c = 2 \sin (k_c d/2)/d$, the second term represents the single vortex contribution, due to Josephson coupling and the last term is due to magnetic couplings ($\tilde{\kappa}_1$ and $\tilde{\kappa}_2$ involve complicated cutoffs) [131]. The replacement of k_c by $\tilde{k}_c$ softens the tilt modulus for short scale distortions along z, and the last term dominates for all k_c if $\Gamma > \lambda_{ab}/d$, i.e. for extreme anisotropies ($\lambda_J > \lambda_{ab}$). This formulation allows in principle to obtain the elastic coefficients for any Γ, but its validity may be questioned for local 2D vortex displacements, shorter than λ_J, for which the dominant interactions are magnetic and are poorly described by a linear theory. This problem deserves a more detailed analysis and is relevant for melting or depinning in Bi : 2212 or multilayers. A more detailed analysis can be found in reference [130]. For instance, the single line tilt modulus ($H = H_{c1}$) is found to be equal to $C_{44}^{IS}[\Gamma^{-2} + (d/\lambda_{ab})^2]$ where C_{44}^{IS} is the isotropic tilt modulus. Thus it is dominated by the dipolar interactions (second term in the bracket) when $\lambda_J > \lambda_{ab}$ (extreme anisotropies).

The results of the linear analysis can be summarized as follows [131] : two distinct regimes appear, determined by the crossover field

$$B_{cr} \approx 2 \pi \frac{\Phi_0}{\lambda_J^2} \text{Ln} \frac{\lambda_J}{\xi_{ab}} \quad (47)$$

characterized by a vortex spacing of the order of λ_J.If $B \ll B_{cr}$, the transverse elasticity is dominated by long scales and the concept of flux lines remains valid, which means that crossing of lines by exchange of 2D vortices is exceptional (Fig. 20a, b). The interlayer coupling is strong, the melting transition is dominated by 3D fluctuations, as in the 3D London description, and corresponds to vanishing of shear stiffness C_{66}, while the interlayer coupling, thus the tilt coefficient C_{44}, remains finite. $T_m(B)$ is given by equation (31) to logarithmic accuracy. A second transition follows, corresponding to vanishing of C_{44}, or in other terms of interlayer coupling. This is the « evaporation » of vortex lines [121], at a temperature $T_{ev} \approx T_m(B_{cr}/B)^{1/2}$

On the opposite, if $B > B_{cr}$, one never reaches the 3D melting, since mutual crossing and exchange dominate [67]. The concept of vortex line looses its meaning and one has 2D vortex lattices in each layer, weakly coupled to each other. The transition temperature is due to 2D fluctuations and is close to that of a single layer (Eq. (45)), with C_{44} and C_{66} vanishing simultaneously at T_m. One passes from a 3D lattice at low temperatures to independent 2D hexatic vortex lattices in each layer [131] (Fig. 20a-c). Such a vortex state has been observed in decoration experiments in Bi : 2212 where B_{cr} is less than 0.1T [133]. One must remark that even below T_m, fluctuations quickly destroy long-range superconducting order along the field direction.

The two limiting situations just described can be understood by defining above T_M a « coherence length » L_c for a given vortex line, as the average distance on which a line of 2D vortices remains distinct from neighbouring ones, before exchanging 2D vortices with them. Given the coefficients C_{44} and C_{66}, it can be written $L_c \approx a_0(C_{44}/C_{66})^{1/2}$ The crossover field B_{cr} can be interpreted as follows : if $B \ll B_{cr}$, $L_c \gg d$ and vortex lines are well-defined. On the other hand, if $B > B_{cr}$, $L_c < d$ and 2D vortices become uncorrelated in different layers.

For a field parallel to the layers, the situation involves a strong anisotropy at low temperatures where out-of-plane vortex fluctuations are frozen by the core barrier. In the

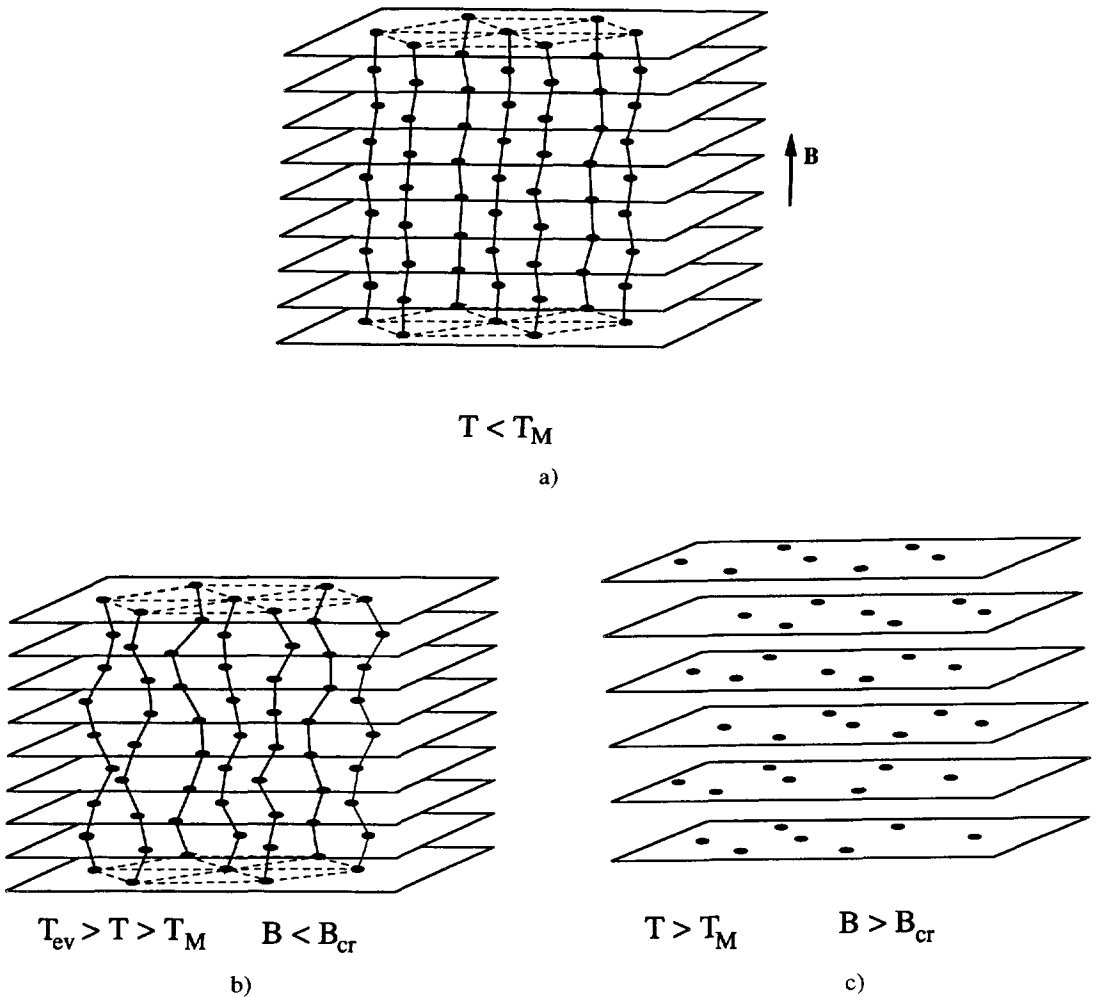

Fig. 20. — Melting of the vortex lattice in a quasi-2D superconductor. a) $T < T_m$, well-defined lines of 2D vortices are ordered in a 3D lattice ; b) $T_{ev} > T > T_m$ (case $B < B_{cr}$), liquid of 2D vortex lines ; c) $T > T_m$ (case $B > B_{cr}$), uncorrelated and melted lattices of 2D vortices in each layer.

remaining one-dimensional fluctuation problem, melting of the parallel vortex lattice might lead at T_m to a two-dimensional superconducting phase with no coherence between layers, first proposed by Efetov in large enough fields [82]. Mikheev and Kolomeisky [134] pointed out that the Lindemann criterium cannot be used, and Korshunov [135], Korshunov and Larkin [136], showed that melting is impossible. They find that the transition is of 3D nature, with $T_{KT} < T_c < T_m$. On the other hand, Horovitz included excitation of 2D vortices. He found the possibility of 2D phase transition in low enough fields, corresponding to an intervortex separation $\ell \geq 8\ d$ across the layers. Let us quote reference [138], where a smectic vortex state is proposed, with zero interlayer shear modulus. Therefore, the phase diagram in parallel fields is complicated, but experiments in progress on multilayers may settle the problem on the experimental point of view.

Conclusion.

This review tries to cover the main intrinsic properties of vortices in layered structures. It focuses principally on the statics of vortices, the dynamics being fundamentally a function of pinning by various defects. However, the role of intrinsic pinning by the layers was mentioned, with the corresponding critical currents. Due to the limited length of the paper, many important properties have not been discussed.

For instance, the nucleation of vortices at a surface (Bean-Livingston barriers [17, 162]) is deeply influenced by the quasi-2D nature of vortices. For fields parallel to the layers it may directly probe the Josephson core and the crossover at T^* [163]. In normal fields, thermal nucleation of 2D vortices provides an easy entrance of vortex lines [164]. Some experiments show evidence for surface barriers in cuprates superconductors [165, 166].

More generally, boundary effects or sample shape can be strong perturbations and must be taken into account in interpreting experiments, in order to probe true bulk properties of the vortex lattice.

The dynamics of vortices in an ac field have been considered for instance by Brandt [167], Coffey and Clem [168], Artemenko and Wonneberger [169]. The nonlocality of vortex interactions, the anisotropy or quasi-2D character are here also essential features of the response.

Little has been said about inertial effects of vortices in junctions, more exactly underdamped motion of vortices in planar junctions separating superconducting layers [12, 146]. More theoretical work, and also experiments in extremely good crystals or films are required to explore this field, especially all the effects coming from the presence of a natural lattice of extended junctions in these systems (see Ref. [171]).

Fluctuation effects, quite important in high-T_c superconductors, would deserve a full separate discussion. While the case of an anisotropic 3D system can be treated with the help of the scaling transformation (Sect. 1.4), quasi-2D fluctuations and the crossover from $3D(T \geqslant T_c)$ to $2D(T \gg T_c)$ fluctuations needs a more elaborate analysis.

The LD model, exploited in section 2, oversimplifies the real layered structure. The description of actual interlayer coupling and proximity effects has received some attention, but needs more microscopic insight and can also lead to unexpected macroscopic effects. Also, a microscopic description of the interlayer Josephson effect is useful to improve the phenomenological models.

To summarize the main features of vortices in layered superconductors, one may say that there is no universal definition of a 3D or 2D behaviour. In fact, provided the interlayer coupling is weak enough, so that the parameter ρ is less than one, many dimensional crossovers can be met, depending on the various physical properties concerned in experiments. To each property one can associate a length scale L_P^c along the c-direction, and, due to anisotropy, a length $L_P^{ab} = \Gamma L_P^c$ along the layer direction. The behaviour will be quasi-3D (resp. quasi-2D) if $L_P^c > d$ or $L_P^{ab} > \lambda_J$ (resp. $L_P^c < d$, or $L_P^{ab} < \lambda_J$). Let us give some examples.

The first (and smallest) characteristic length is the GL coherence length, $\xi_{ab} = \Gamma \xi_c$. It gives rise to the crossover temperature T^*, which concerns the critical field H_{c2}, the core structure (staircase vortices, lock-in, surface barrier for nucleation of a vortex parallel to the layers), and also the fluctuations above the H_{c2} line. It may also concern some pinning mechanisms when the range of pinning potential is small and in case of strong pinning. The best example is intrinsic pinning but some strong pinning centers may lead to a similar analysis. Note that even in Y : 123 which is mostly 3D, quasi-2D effects as the lock-in transition exist. The core structure in the quasi-3D region $T^* < T < T_c$ still reflects the layered structure.

A second characteristic length is the London length λ_{ab}. If $\lambda_{ab} < \lambda_J$, the case of extreme

anisotropy, nearly all relevant lengths in the layers will be smaller than λ_J and the corresponding system properties are basically 2D. However, at very low temperatures, the magnetic couplings correlate the vortex structure in different layers and a certain 3D character should be present, though difficult to probe experimentally. In tilted fields, the tilted Abrikosov lattice would be replaced by a « combined » lattice made of interpenetrating vortex lattices along the c- and layer directions. The thermodynamics of such extremely weakly coupled layered structures are dominated by vortex and fluxon fluctuations.

In the Abrikosov lattice of 2D vortices, vortex lines can still be defined below the melting transition T_M. Above T_M, this is possible only on a correlation length L_c, and if $L_c > d$. The dimensional crossover in this case corresponds roughly to $a_0 \approx \lambda_J$.

The generalization of this rich phenomenology to quasi-one dimensional structures is an important problem. Moreover, experiments on lower-T_c materials may better isolate the contributions of anisotropy and short coherence length from those of high T_c, leading to strong fluctuations. From the experimental point of view, only volume probes of the vortex state could unambiguously and directly provide evidences for the unusual structure of the vortex « matter » in layered materials.

Acknowledgements.

The author is indebted to Prof. Friedel for triggering his interest in the field, and acknowledges L. Bulaevskii, A. Buzdin, L. Fruchter, Ø. Fischer, P. Manuel, P. Monceau, S. Senoussi, S. Theodorakis, R. Tournier and J. M. Triscone for useful discussions.

References

[1] Sleight A. W., Gilson J. L. and Bierstedt P. E., *Solid State Commun.* **17** (1975) 27.
[2] Cava R. J., Batlogg B., Krajewski J., Ferrel R. C., Rupp L. W., White A. E., Peck W. F. and Kometani T. W., *Nature* **332** (1988) 814.
[3] Armici J. C., Decroux M., Fischer Ø., Potel M., Chevrel R. and Sergent M., *Solid State Commun.* **33** (1980) 607.
[4] Hebard A. F., Rosseinsky M. J., Haddon R. C., Murphy D. W., Glarum S. H., Palstra T. T. M., Ramirez A. P. and Kortan A. R., *Nature* **350** (1991) 600.
[5] For a review see Bulaevskii L. N., *Usp. Fiz. Nauk* **116** (1975) 449 [*Sov. Phys. Usp.* **18** (1976) 514].
[6] For reviews on organic superconductors, see Low Dimensional Conductors and Superconductors, NATO-ASI, D. Jérome and L. Caron Eds., Vol. **55** (Plenum Press, N.Y., 1987) and Proceedings of the Int. Conf. on Science and Technology of Synthetic Metals 1988 (Synth. Mat. 27, 1, 2 (1988)).
[7] Koike Y., Suematsu H., Higuchi K. and Tanuma S., *Physica* **B 99** (1980) 503.
[8] Triscone J. M., Karkut M. G., Antognazza L., Brunner O. and Fischer Ø., *Phys. Rev. Lett* **63** (1989) 1016.
[9] Satoh T., Fujita J., Yoshitake T., Igarashi H., Miura S., Matsukura N. and Tsuge H., *Physica* **C 185-189** (1991) 2059.
[10] Li Q., Xi X. X., Wu X. D., Inan A., Vadlamannati S., Mc Lean W. L., Venkatesan T., Ramesh R., Hwang D. M., Martinez J. A. and Nazar L., *Phys. Rev Lett.* **64** (1990) 3086.
[11] Escribe-Filippini C., Beille J., Boujida M., Marcus J. and Schlenker C., *Physica* **C 162-164** (1989) 427.
[12] Bulaevskii L. N., *Int. J. Mod. Phys.* **B 4** (1990) 1849 (a review).
[13] De Rango P., Giordanengo B., Tournier R., Sulpice A., Chaussy J., Deutscher G., Genicon J. L., Lejay P., Retoux R. and Raveau B., *J. Phys. France* **50** (1989) 2857.
[14] Theodorakis S. and Tesanovic Z., *Phys. Rev.* **B 40** (1989) 6659.
[15] Koyama T., Takezawa N. and Tachiki M., *Physica* **C 168** (1990) 69.
[16] Theodorakis S. and Feinberg D., *Physica* **C 190** (1992) 271.

[17] de Gennes P. G., Superconductivity of Metals and Alloys (Benjamin, 1966).
[18] Lawrence W. E. and Doniach S., Proc. of the 12th Conf. on Low-Temperature Physics, Kyoto 1970, E. Kanda Ed. (Keigaku, 1970) p. 361.
[19] Bulaevskii L. N., *Zh. Eksp. Teor. Fiz.* **64** (1973) 2241 [*Sov. Phys. JETP* **37** (1973) 1133].
[20] Feinberg D. and Villard C., *Mod. Phys. Lett.* **B 4** (1990) 9 ; *Phys. Rev. Lett.* **65** (1990) 919 ; Feinberg D., *Solid State Commun.* **76** (1990) 789. In the last two papers the nonlocality of the elastic tilt modulus was not treated properly, leading to incorrect field dependence of the lock-in angle and kink length.
[21] Feinberg D. and Ettouhami A. M., *Int. J. Mod. Phys. B*, in press (1993) (a review).
[22] Senoussi S., *J Phys. III France* **2** (1992) 1041.
[23] Landau L. and Ginzburg V. L., *Zh. Eksp. Teor. Fis.* **20** (1950) 1064 ; Ginzburg V. L., *Zh. Eksp. Teor. Fiz.* **23** (1952) 236.
[24] Abrikosov A. A., *Zh. Eksp. Teor. Fis.* **32** (1957) 1442 [*Sov. Phys. JETP* **5** (1957) 1174].
[25] Balatskii A. V., Burlachkov L. I. and Gor'kov L. P., *Zh. Eksp. Teor. Fiz.* **90** (1986) 1478 [*Sov. Phys JETP* **63** (1986) 866].
[26] Klemm R. A. and Clem J. R., *Phys. Rev.* **B 21** (1980) 1868 ; Klemm R. A., *Phys. Rev.* **B 38** (1988) 6641.
[27] Buzdin A. I. and Simonov A. Yu., *Pis ma Zh. Eksp. Teor. Fiz.* **51** (1990) 168 [*JETP Lett.* **51** (1990) 191] ; Grishin A. M., Martynovich A. Yu. and Yampol'skii S. V., *Zh. Eksp. Teor. Fiz.* **97** (1990), 1930 [*Sov. Phys. JETP* **70** (1990), 1089] ; Kogan V. G., Nakagawa N. and Thiemann S. L., *Phys. Rev.* **B 42** (1990), 2631.
[28] Buzdin A. I. and Simonov A. Yu., *Physica* **C 175** (1991) 143.
[29] Gammel P. L., Bishop D. J., Rice J. P. and Ginsberg D. M., *Phys. Rev. Lett.* **68** (1992) 3343.
[30] Kogan V. G., *Phys. Lett.* **85A** (1981) 299 ; Campbell L. J., Doria M. M. and Kogan V. G., *Phys. Rev.* **B 38** (1988) 2439.
[31] Dolan G. J., Holtzberg F., Feild C. and Dinger T. R., *Phys. Rev. Lett.* **62** (1989) 2184.
[32] Hess H. F., Murray C. A. and Waszczak J. V., *Phys. Rev. Lett.* **69** (1992) 2138.
[33] Ivlev B. I., Kopnin N. B. and Salomaa M. M., *Phys. Rev.* **B 43** (1991) 2896.
[34] Ivlev B. I. and Kopnin N. B., *Phys. Rev.* **B 44** (1991) 2747.
[35] Sudbø A. and Brandt E. H., *Phys. Rev. Lett.* **68** 1758 ; Chui S. T., *Solid State Commun.* **83** (1992) 441.
[36] Bolle C. A., Gammel P. L., Grier D. G., Murray C. A., Bishop D. J., Mitzi D. B. and Kapitulnik A., *Phys. Rev Lett.* **66** (1991) 112.
[37] Sudbø A., *Physica* **C 201** (1992) 369.
[38] Bulaevskii L. N., Ledvij M. and Kogan V. G., *Phys. Rev* **B 46** (1992) 366.
[39] Feinberg D., *Physica* **C 194** (1992) 126 ; Proceedings of the Vth NYSIS Conference on Superconductivity, Buffalo 1991, Y. H. Kao, A. E. Kaloyeros and H. S. Kwok Eds. (AIP Publ., 1991) p. 489.
[40] Kogan V. G., *Phys. Rev.* **B 38** (1988) 7049.
[41] Farrell D. E., Williams C. M., Wolf S. A., Bansal N. P. and Kogan V. G., *Phys. Rev. Lett.* **61** (1988) 2805.
[42] Janossy B., Prost D., Pekker S. and Fruchter L., *Physica* **C 181** (1991) 51.
[43] Tuominen M., Goldman A. M., Chang Y. Z. and Jiang P. Z., *Phys. Rev.* **B 42** (1990) 412.
[44] Farrell D. E., Bonham S., Foster J., Chang Y. C., Ziang P. Z., Vandervoort K. G., Lam D. J. and Kogan V. G., *Phys. Rev. Lett.* **63** (1989) 782.
[45] Okuda K., Kawamata S., Noguchi S., Itoh N. and Kadowaki K., *J. Phys. Soc. Jpn* **60** (1991) 3226.
[46] Martinez J. C., Brongersma S. H., Koshelev A., Ivlev B., Kes P. H., Griessen R. P., de Groot D. G., Tarnavski Z. and Menovsky A. A., *Phys. Rev. Lett.* **69** (1992) 2276.
[47] Fruchter L., Janossy B. and Campbell I. A., Proc. of the 12th European Physical Society Conference (Prague, 1992).
[48] Blatter G., Geshkenbein V. B. and Larkin A. I., *Phys. Rev. Lett.* **68** (1992) 875.
[49] Zhidong Hao and Clem J. R., *Phys. Rev.* **B 46** (1992) 5853.

[50] Kogan V. G. and Clem J. R., *Phys. Rev.* **B 24** (1981) 2497.
[51] Buzdin A. and Feinberg D., *Physica C*, in press.
[52] Kes P. H., Aarts J., Vinokur V. M. and van der Beek C. J., *Phys. Rev. Lett.* **64** (1990) 1063.
[53] Raffy H., Labdi S., Laborde O. and Monceau P., *Phys. Rev. Lett.* **66** (1991) 2515.
[54] Brandt E. H., *Physica* C **195** (1992) 1 ; *Int. J. Mod. Phys.* **B 5** (1991) 751 (reviews).
[55] Brandt E. H. and Essmann U., *Phys. Status Solidi* **B 144** (1987) 13 (a review).
[56] Brandt E. H. and Sudbø A., *Phys. Rev. Lett.* **66** (1991) 2278 ;
Sudbø A. and Brandt E. H., *Phys. Rev. Lett* **67** (1991) 3176.
[57] Brandt E. H., *J. Low Temp. Phys* **26** (1977) 709, 735.
[58] Sudbø A. and Brandt E. H., *Phys. Rev* **B 43** (1991) 10482.
[59] Sardella E., *Phys. Rev.* **B 45** (1992) 3141.
[60] Houghton A., Pelcovits R. A. and Sudbø A., *Phys. Rev.* **B 40** (1989) 6763.
[61] Sudbø A. and Brandt E. H., *Phys. Rev. Lett.* **66** (1991) 1781 ;
Brandt E. H. and Sudbø A., *Physica* C **180** (1991) 426.
[62] Kogan V. G. and Campbell L. J., *Phys. Rev. Lett.* **62** (1989) 1552.
[63] Buisson O., Carneiro G. and Doria M., *Physica* C **185-189** (1991) 1465 ;
Marchetti M. C., *Physica* C **200** (1992) 155.
[64] Huse D. A., *Phys. Rev.* **B 46** (1992) 8621.
[65] Nelson D. R., *Phys. Rev. Lett.* **60** (1988) 1973 ;
Nelson D. R. and Seung H. S., *Phys. Rev* **B 39** (1989) 9153.
[66] Brandt E. H., *Phys. Rev. Lett.* **63** (1989) 1106.
[67] Doniach S., High Temperature Superconductivity, Los Alamos Symposium 1989, K. S. Bedell, D. Coffey, D. E. Meltzer, D. Pines and J. R. Schrieffer Eds. (Addison Wesley, Redwood City, 1990) p. 406.
[68] Fisher D. S., Fisher M. P. A. and Huse D. A., *Phys. Rev.* **B 43** (1991) 130 (a review).
[69] Feigelman M. V., *Physica* **A 168** (1990) 319 ;
Feigelman M. V., Geshkenbein V. B. and Vinokur V. M., *Pisma Zh. Eksp. Teor. Fiz.* **52** (1990) 1141 [*JETP Lett.* **52** (1990) 547].
[70] Fisher M. P. A., *Phys. Rev. Lett.* **62** (1989) 1415.
[71] Koch R. M., Foglietti V., Gallagher W. J., Koren G., Gupta A. and Fisher M. P. A., *Phys. Rev. Lett.* **63** (1989) 1511.
[72] Giura M., Marcon R., Silva E. and Fastampa R., *Phys. Rev.* **B 46** (1992) 5753.
[73] Safar H., Gammel P. L., Huse D. A., Bishop D. J., Rice J. P. and Ginsberg D. M., *Phys. Rev. Lett.* **69** (1992) 824.
[74] Farrell D. E., Rice J. P. and Ginsberg D. M., *Phys Rev. Lett.* **67** (1991) 1165.
[75] Charalambous M., Chaussy J. and Lejay P., *Phys. Rev.* **B 45** (1992) 5091.
[76] Worthington T. K., Fisher M. P. A., Huse D. A., Toner J., Marwick A. D., Zabel T., Feild C. A. and Holtzberg F., *Phys. Rev.* **B 46** (1992) 11854.
[77] Kwok W. K., Fleshler S., Welp U., Vinokur V. M., Downey J. and Crabtree G. W., *Phys. Rev. Lett.* **69** (1992) 3370.
[78] Koyama T., Takezawa N., Naruse Y. and Tachiki M., *Physica* C **194** (1992) 20 ;
Feinberg D., Theodorakis S. and Ettouhami A. M., *Phys Rev. B* (in press).
[79] Feigelman M. V., Geshkenbein V. B. and Larkin A. I., *Physica* C **167** (1990) 177.
[80] Artemenko S. N. and Kruglov A. N., *Phys. Lett.* **A 143** (1990) 485.
[81] Farrell D. E., Rice J. P., Ginsberg D. M. and Liu J. Z., *Phys. Rev. Lett.* **64** (1990) 1573.
[82] Efetov K. B., *Zh. Eksp Teor. Fiz* **76** (1979) 1781 [*Sov. Phys Phys. JETP* **49** (1979) 905].
[83] Buzdin A. and Feinberg D., *J. Phys. France* **51** (1990) 1971.
[84] Guinea F., *Phys. Rev.* **B 42** (1990) 6244.
[85] Clem J. R., *Phys. Rev.* **B 43** (1991) 7837.
[86] Fischer K. H., *Physica* C **178** (1991) 161.
[87] Pearl J., *Appl. Phys. Lett.* **5** (1964) 65.
[88] Iye Y., Tamegai T. and Nakamura S., *Physica* C **174** (1991) 227 ;
Iye Y., Terashima T. and Bando Y., *Physica* C **177** (1991) 393.
[89] Carton J. P., *J. Phys. I France* **1** (1991) 113.

[90] Friedel J., *Physica C* **153-155** (1988) 610 ;
Friedel J., *J. Phys. Condensed Matter* **1** (1989) 7757.
[91] Koyama T., Takezawa N. and Tachiki M., *Physica* C **172** (1991) 501.
[92] Clem J. R. and Coffey M. W., *Phys. Rev.* **B 42** (1990) 6209 ;
Clem J. R., Coffey M. W. and Hao Zhidong, *Phys. Rev.* **B 44** (1991) 2732.
[93] Bulaevskii L. N. and Clem J. R., *Phys. Rev.* **B 44** (1991) 10234.
[94] Klemm R. A., Beasley M. R. and Luther A., *J. Low Temp. Phys.* **16** (1974) 607.
[95] Burkov S. E., *Phys. Rev.* **B 44** (1991) 2850.
[96] Bulaevskii L. N., *Phys. Rev.* **B 44** (1991) 910.
[97] Ivlev B. I., Ovchinnikov Yu. I. and Pokrovsky V. L., *Europhys. Lett.* **13** (1990) 187 ; *Mod. Phys. Lett.* **B 5** (1991) 73.
[98] Deutscher G. and Entin-Wohlmann O., *Phys. Rev. B* **17** (1993) 1249.
[99] Maslov S. S. and Pokrovsky V. L., *Europhys. Lett.* **14** (1991) 591.
[100] Koshelev A. E., *Phys. Rev. B* **48** (1993) 1180.
[101] Chung O. H., Chaparala M. and Naughton M. J., Proceedings of the VIth NYSYS Conference on Superconductivity, Sept. 1992, Buffalo (AIP, 1993) ;
Naughton M., private communication.
[102] Martinez J. C., Brongersma S. H., Koshelev A. E., Ivlev B., Kes P. H., Griessen R. P., de Groot D. G., Tarnavski Z. and Menovsky A. A., *Phys. Rev. Lett.* **69** (1992) 2276.
[103] Kwok W. K., Welp U., Vinokur V. M., Fleshler S., Downey J. and Crabtree G. W., *Phys. Rev. Lett.* **67** (1991) 390.
[104] Kosterlitz J. M. and Thouless D. J., *J. Phys.* **C 6** (1973) 1181.
[105] Berezinskii V. L., *Zh. Eksp. Teor. Fiz.* **61** (1971) 1144 [*Sov. Phys. JETP* **34** (1972) 610].
[106] Halperin B. I. and Nelson D. R., *J. Low Temp. Phys.* **36** (1979) 599.
[107] Minnhagen P., *Rev. Mod. Phys.* **59** (1987) 1001 (a review).
[108] Beasley M. R., Mooij J. E. and Orlando T. P., *Phys. Rev. Lett.* **42** (1979) 1165.
[109] Doniach S. and Huberman B. A., *Phys. Rev. Lett.* **42** (1979) 1169 ;
Huberman B. A. and Doniach S., *Phys. Rev. Lett.* **43** (1979) 950.
[110] Stamp P. C. E., Forrò L. and Ayache C., *Phys. Rev.* **B 38** (1988) 2847.
[111] Yeh N. C. and Tsuei C. C., *Phys. Rev.* **B 39** (1989) 9708.
[112] Martin S., Fiory A. T., Fleming R. M., Espinosa G. P. and Cooper A. S., *Phys. Rev. Lett.* **62** (1989) 677.
[113] Kim D. H., Goldman A. M., Kang J. H. and Kampwirth R. T., *Phys. Rev.* **B 40** (1989) 8834.
[114] Artemenko S. N., Gorlova I. G. and Latyshev Yu. I., *Phys. Lett.* **A 138** (1989) 428 ;
Artemenko S. N. and Latyshev Yu. I., *Mod. Phys. Lett.* **B 6** (1992) 367.
[115] Norton D. P., Lowndes D. H., Zheng Z. Y., Feenstra R. and Zhu Shen, Proceedings of the Vth Conference on Superconductivity, Buffalo 1991, Y. H. Kao, A. E. Kaloyeros and H. S. Kwok Eds. (AIP Publ., 1991) p. 33.
[116] Horovitz B., *Phys. Rev. Lett.* **67** (1991) 378 ; **145** (1992) 12632 ; *Phys. Rev. B* **47** (1993) 5955.
[117] Scheidl S. and Hackenbroich G., *Europhys. Lett.* **20** (1992) 511 ; *Phys. Rev.* **B 46** (1992) 14010.
[118] Bulaevskii L. N., Meshkov S. V. and Feinberg D., *Phys. Rev.* **B 43** (1991) 3728.
[119] Artemenko S. N. and Kruglov A. N., *Physica* C **173** (1991) 125.
[120] Hackenbroich G. and Scheidl S., *Physica* C **181** (1991) 163.
[121] Bulaevskii L. N., Ledvij M. and Kogan V. G., *Phys. Rev. Lett.* **68** (1992) 3773.
[122] Friedel J., *J. Phys. France* **49** (1988) 1561.
[123] Korshunov S. E., *Europhys. Lett.* **11** (1990) 757.
[124] Triscone J. M., Fischer Ø., Brunner O., Antognazza L., Kent A. D. and Karkut M. G., *Phys. Rev. Lett.* **64** (1990) 804.
[125] Rasolt M., Edis T. and Tesanovic Z., *Phys. Rev. Lett.* **66** (1991) 2927.
[126] Wood R. F., *Phys. Rev. Lett.* **66** (1991) 829.
[127] Lowndes D. H., Norton D. P. and Budai J. D., *Phys. Rev. Lett.* **65** (1990) 1160.
[128] Terashima T., Shimura K., Bando Y., Matsuda Y., Fujiyama A. and Komiyama S., *Phys. Rev. Lett.* **67** (1991) 1362.
[129] Fisher D. S., *Phys. Rev.* **B 22** (1980) 1190.

[130] Fischer K. H., *Physica* C **193** (1992) 401.
[131] Glazman L. I. and Koshelev A. E., *Physica* C **173** (1991) 180 ; *Phys. Rev.* B **43** (1991) 2835.
[132] Forgan E. M., *Physica* C **185-189** (1991) 247 ;
Yethiraj M., Mook H. A., Wignall G. D., Cubitt R., Forgan E. M., Paul D. M. and Armstrong T., *Phys. Rev. Lett.* **70** (1993) 857.
[133] Grier D. G., Murray C. A., Bolle C. A., Gammel P. L., Bishop D. J., Mitzi D. B. and Kapitulnik A., *Phys. Rev. Lett.* **66** (1991) 2270.
[134] Mikheev L. V. and Kolomeisky E. B., *Phys. Rev.* B **43** (1991) 10431.
[135] Korshunov S. E., *Europhys. Lett.* **15** (1991) 771.
[136] Korshunov S. E. and Larkin A. I., *Phys. Rev.* B **46** (1992) 6395.
[137] Barone A., Larkin A. I. and Ovchinnikov Yu. N., *J. Supercond.* **3** (1990) 155.
[138] Blatter G., Ivlev B. I. and Rhyner J., *Phys. Rev. Lett.* **66** (1991) 2392.
[139] Minenko E. V. and Kulik I. O., *Fiz. Nizk. Temp.* **5** (1979) 1237 [*Sov. J. Low Temp. Phys.* **5** (1979) 583].
[140] Tachiki M. and Takahashi S., *Solid State Commun.* **72** (1989) 1083.
[141] Roas B., Schultz L. and Saemann-Ischenko G., *Phys. Rev. Lett.* **64** (1990) 479.
[142] Theodorakis S., *Phys. Rev.* B **42** (1990) 10172.
[143] Deutscher G. and Kapitulnik A., *Physica* A **168** (1990) 338.
[144] Wu J. Z., Ting C. S., Chu W. K. and Yao X. X., *Phys. Rev.* B **44** (1991) 411.
[145] Safar H., Rodriguez E., de la Cruz F., Gammel P. L., Schneemeyer L. F. and Bishop D. J., *Phys. Rev.* B **46** (1992) 14238.
[146] Coffey M. W. and Clem J. R., *Phys. Rev.* B **44** (1991) 6903.
[147] Vinokur V. M., Feigelman M. V., Geshkenbein V. B. and Larkin A. I., *Phys. Rev. Lett.* **65** (1990) 259.
[148] Ivlev B. I. and Kopnin N. B., *J. Low Temp. Phys.* **77** (1989) 413 ; **80** (1990) 161.
[149] Ivlev B. I. and Kopnin N. B., *Phys. Rev.* B **42** (1990) 10052.
[150] Chakravarty S., Ivlev B. I. and Ovchinnikov Yu. N., *Phys. Rev.* B **42** (1990) 2143 ; *Phys. Rev. Lett.* **64** (1990) 3187.
[151] Ivlev B. I. and Kopnin N. B., *Europhys. Lett.* **15** (1991) 349 ;
Ovchinnikov Yu. N. and Ivlev B. I., *Phys. Rev.* B **43** (1991) 8024.
[152] Pokrovsky V. L., Lyuksyutov I. and Nattermann T., *Phys. Rev.* B **46** (1992) 3071.
[153] Iye Y., Nakamura S., Tamegai T., Terashima T., Yamamoto K. and Bando Y., *Physica* C **166** (1990) 62.
[154] Ivlev B. I., Ovchinnikov Yu. N. and Thompson R. S., *Phys. Rev.* B **44** (1991) 7023.
[155] Blatter G., Geshkenbein V. M. and Vinokur V. M., *Phys. Rev. Lett.* **66** (1991) 3297.
[156] Minnhagen P., *Solid State Commun.* **71** (1989) 25 ;
Jensen H. J. and Minnhagen P., *Phys. Rev. Lett.* **66** (1991) 1630.
[157] Tinkham M., Introduction to Superconductivity (MacGraw-Hill, 1975), Chapt. 5.
[158] Naughton M. J., Yu R. C., Davies P. K., Fischer J. E., Chamberlin R. V., Wang Z. Z., Jing T. W., Ong N. P. and Chaikin P. M., *Phys. Rev.* B **38** (1988) 9280.
[159] Bauhofer W., Biberacher W., Gegenheimer B., Joss W., Kremer R. K., Mattausch H., Müller A. and Simon S., *Phys. Rev. Lett.* **63** (1989) 2520.
[160] Fastampa R., Giura M., Marcon R. and Silva E., *Phys. Rev. Lett.* **67** (1991) 1795.
[161] Braithwaite D., Bourgault D., Sulpice A., Barbut J. M., Tournier R., Monot I., Lepropre M., Provost J. and Desgardin G., *J. Low Temp. Phys.* **91** (1993) 1.
[162] Bean C. P. and Livingston J. B., *Phys. Rev. Lett.* **12** (1964) 14.
[163] Buzdin A. and Feinberg D., *Phys. Lett.* A **165** (1992) 281.
[164] Buzdin A. and Feinberg D., *Phys. Lett.* A **167** (1992) 89.
[165] Kopylov V. N., Koshelev A. E., Schegolev I. F. and Togonidze T. G., *Physica* C **170** (1990) 291.
[166] Konczykowski M., Burlachkov L. I., Yeshurun Y. and Holtzberg F., *Phys. Rev.* B **43** (1991) 13707.
[167] Brandt E. H., *Phys. Rev. Lett.* **67** (1991) 2219.
[168] Coffey M. W. and Clem J. R., *Phys. Rev. Lett.* **67** (1991) 386.
[169] Artemenko S. N. and Wonneberger W., *Physica* C **192** (1992) 453.

[170] Fruchter L., Malozemoff A. P., Campbell I. A., Sanchez J., Konczykowski M., Griessen R. and Holtzberg F., *Phys. Rev.* **B 43** (1991) 8709.
[171] Kleiner R., Steinmeyer F., Kunkel G. and Müller P., *Phys. Rev. Lett.* **687** (1992) 2394.
[172] Mansky P. A., Chaikin P. M. and Haddon R. C., *Phys. Rev. Lett.* **70** (1993) 1323.
[173] Gabay M. and Kapitulnik A., *Phys. Rev. Lett.* **71** (1993) 2138 ;
Shou-Cheng Zhang, *Phys. Rev. Lett.* **71** (1993) 2142.
[174] Horovitz B., *Phys Rev. B* **47** (1933) 5964.